UNIVERSITY OF CALIFORNIA

Los Angeles

Investigating Nucleotide Deficiency-Based Genomic Instability and CRISPR/Cas9-mediated Genomic Addition for the Therapeutic Applications of Human Induced Pluripotent Stem Cells

A dissertation submitted in partial satisfaction of the requirements for the degree

Doctor of Philosophy

in Molecular and Medical Pharmacology

by

Patrick Chris Lee

2016

ABSTRACT OF THE DISSERTATION

Investigating Nucleotide Deficiency-Based Genomic Instability
and CRISPR/Cas9-mediated Genomic Addition for the Therapeutic Applications of
Human Induced Pluripotent Stem Cells

by

Patrick Chris Lee
Doctor of Philosophy in Molecular and Medical Pharmacology
University of California, Los Angeles, 2016
Professor Gerald S. Lipshutz, Chair

Since the first reported generation of induced pluripotent stem cells (hiPSCs) from human somatic cells, the stem cell field has emerged as a promising avenue for both modeling and treating diseases[1,2]. The difficulty in obtaining primary cell cultures has hindered the progress of disease research. Since patient-specific hiPSCs can be derived from accessible sources, such as dermal fibroblasts, and can differentiate into specialized cell types, it is possible to generate a substantial quantity of these patient-specific cells to overcome this obstacle[3,4]. Furthermore, recent advances in genetic modification of hiPSCs make the goal of autologous cell transplantation even more attainable.

However, there are still numerous obstacles, such as genomic instability, that impede the translation of stem cell technology to clinical applications.

Nucleoside supplementation restores dNTP pools and alleviates genomic instability in hiPSCs

hiPSCs acquire genetic alterations, such as aneuploidy, through the reprogramming process and extensive passaging, jeopardizing their translation to clinical applications. We report that hiPSCs have an imbalance of deoxynucleotide triphosophate (dNTP) pools, which are required for DNA synthesis, potentially inducing replicative stress in hiPSCs. Additionally, hiPSCs exhibit higher levels of double-stranded breaks, indicating greater incidence of DNA damage. We demonstrate that genomic damage in hiPSCs can be alleviated when the cells are cultured with exogenous nucleosides, utilizing the cell's nucleotide salvage pathway (NSP) to augment endogenous dNTP pools.

Restoring ureagenesis in hepatocytes by CRISPR/Cas9-mediated genomic addition to arginase-deficient induced pluripotent stem cells

Urea cycle disorders are incurable enzymopathies that affect nitrogen metabolism and typically lead to hyperammonemia. Arginase deficiency results from a mutation in Arg1, the enzyme regulating the final step of ureagenesis and typically results in developmental disabilities, seizures, spastic diplegia, and sometimes death. Current medical treatments for urea cycle disorders are only marginally effective, and for proximal disorders, liver transplantation is effective but limited by graft availability.

Advances in human induced pluripotent stem cell research have allowed for the genetic modification of stem cells for potential cellular replacement therapies. We demonstrate a CRISPR/Cas9-based strategy utilizing exon 1 of the hypoxanthine-guanine phosphoribosyltransferase (HPRT) locus to genetically modify and restore arginase activity, and thus ureagenesis, in genetically distinct patient-specific human induced pluripotent stem cells and hepatocyte-like derivatives. Successful strategies restoring gene function in patient-specific human induced pluripotent stem cells may advance applications of genetically modified cell therapy to treat urea cycle and other inborn errors of metabolism.

The dissertation of Patrick Chris Lee is approved.

Samson A. Chow

Harvey R. Herschman

Caius Gabriel Radu

Stephen D. Cederbaum

Gerald S. Lipshutz, Committee Chair

University of California, Los Angeles

2016

My doctoral work is dedicated to my parents, Chris and Jenny Lee, who have been stalwart supporters of me throughout my academic career.

TABLE OF CONTENTS

LIST OF TABLES AND FIGURES

BIOGRAPHICAL SKETCH

Education

University of California, Berkeley August 2005 - May 2009
B.A. Molecular and Cell Biology - Neurobiology

Professional Experience

Stanford University School of Medicine January 2010 – June 2012
Life Science Research Assistant
Institute of Stem Cell Biology and Regenerative Medicine – Reijo Pera Lab

Genentech, Inc. June 2009 – September 2009
Research Intern – Feierbach Lab
Department of Microbial Pathogenesis – Feierbach Lab

Honors and Awards

Regents' and Chancellor's Scholarship - University of California, Berkeley 2005
Graduate Dean's Scholar Award - University of California, Los Angeles 2012

Patents

Nucleoside supplementation to promote cellular function, genetic stability, regenerative applications (United States Patent Application 20150105343)
Inventors: James A. Byrne, Caius G. Radu, Patrick C. Lee

Publications

Lee PC, Truong B, Vega-Crespo A, Gilmore WB, Hermann K, Kingman S, Tang JK, Chang KM, Wininger AE, Lam AK, Schoenberg BE, Cederbaum SD, Pyle AD, Byrne JA, Lipshutz GS. Restoring ureagenesis in hepatocytes by CRISPR/Cas9-mediated genomic addition of arginase-deficient induced pluripotent stem cells. *Mol Ther Nucleic Acids* (2016).

Vega-Crespo A, Truong B, Hermann KJ, Awe JP, Chang KM, **Lee PC**, Schoenberg BE, Wu L, Byrne JA, Lipshutz GS. Investigating the functionality of an OCT4-short response element in human induced pluripotent stem cells. *Mol Ther Methods Clin Dev* (2016).

Durruthy-Durruthy J, Briggs SF, Awe J, Ramathal CY, Karumbayaram S, **Lee PC**, Heidmann JD, Clark A, Karakikies I, Loh KM, Wu JC, Hoffman AR, Byrne J, Reijo Pera RA, Sebastiano V. Rapid and efficient conversion of integration-free human induced pluripotent stem cells to GMP-grade culture conditions. *PLoS One* 9(4) (2014).

Awe JP, **Lee PC**, Ramathal C, Vega-Crespo A, Durruthy-Durruthy J, Cooper, AC, Karumbayaram, S, Lowry WE, Clark AT, Zack JA, Sebastiano V, Kohn DB, Pyle AD, Martin MG, Lipshutz GS, Phelps PE, Reijo Pera RA, Byrne, JA. Generation and Characterization of transgene-free human induced pluripotent stem cells and conversion to putative clinical-grade status. *Stem Cell Res Ther* 4(4):87. (2013)

Lee PC and Reijo Pera R. Therapeutic Applications of Induced Pluripotent Stem Cells in Parkinson's Disease. *Stem Cells and Cancer Stem Cells* 6:409-20 (2012)

Byers B, Cord B, Nguyen H, Schule B, Fenno L, **Lee PC,** Deisseroth K, Langston JW, Reijo Pera R, Palmer T. SNCA triplication in iPSC-derived DA neurons accumulate α-Synuclein and are susceptible to oxidative stress. *PLoS ONE* 6(11): e26159 (2011).

Pending Publications

Lee PC, Truong B, Vega-Crespo A, Ciminera A, Tang JK, Schoenberg B, Chang KM, Byrne JA, Lipshutz GS. Nucleoside supplementation restores dNTP balance and alleviates genomic instability in human induced pluripotent stem cells. (2016).

Poster Presentations

Lee PC, Vega-Crespo A, Truong B, Tang JK, Herschman HR, Radu CG, Byrne JA. "Reducing Replicative Stress in Human Induced Pluripotent Stem Cells Enhances Genetic Integrity." Tri-Institutional Stem Cell Retreat of the Eli and Edythe Broad Centers of Regeneration. Asilomar, 2014.

Lee PC, Kim W, Truong B, Le T, Dimitrova E, Herschman HR, Radu CG, Byrne JA. "Reducing Replicative Stress in Human Induced Pluripotent Stem Cells Enhances Genetic Integrity." UCLA Broad Stem Cell Research Center Annual Symposium, Los Angeles, 2014.

Wani P, **Lee PC**, Xia N, and Reijo Pera R. "Generation, Characteration, and Differentiation of Patient Derived Induced Pluripotent Stem Cells toward Dopaminergic Neurons to Model Parkinson's Disease." Stanford University Reproductive and Stem Cell Biology Retreat, Stanford 2012.

Gujar P, Nguyen HN, **Lee PC**, and Reijo Pera R. "Generation of Induced Pluripotent Stem Cell Lines from Patients with Sporadic Form of Parkinson's disease and Reprogramming." Cold Spring Harbor Germ Cell Conference, New York 2010.

Lee PC, Fouts A, and Feierbach B. "Identifying New Receptors for Human Cytomegalovirus (HCMV)." Genentech, South San Francisco, 2009

Introduction to the thesis

Since the first reported generation of induced pluripotent stem cells (hiPSCs) from human somatic cells independently by the labs of Shinya Yamanaka of Kyoto University and James Thomson of the University of Wisconsin-Madison in 2007, the stem cell field has emerged as a promising avenue for both modeling and treating various diseases[1,2]. Whereas the difficulty in obtaining certain primary cell cultures has hindered the progress of disease research, the ability to derive hiPSCs from human dermal fibroblasts and differentiate them into various specific cell types, such as neurons and hepatocytes, provide the advantage of generating a substantial quantity of these patient-specific cell types to overcome this obstacle[3,4]. In 2013, the RIKEN Center for Developmental Biology announced the first pilot clinical study using hiPSCs as a cell-replacement therapeutic by transplanting autologous hiPSC-derived retinal pigment epithelium (RPE) cells into patients suffering from age-related macular degeneration (AMD), thus highlighting the progress of translating hiPSC technology to clinical applications and advancing personalized medicine[5].

Advancements in genetic engineering utilizing clustered regularly interspaced short palindromic repeats (CRISPR)/ Cas9 system has made the ability to modify and correct patient-specific disease hiPSCs more efficient[6,7,8,9]. The CRISPR/Cas9 system is inspired by the prokaryotic immune system in which foreign genetic elements are recognized by CRISPR spacers and are excised out of the bacterial genome[10]. Custom spacer sequences can be transcribed into short RNA sequences and can guide the CRISPR system to matching DNA sequences in human cells and cut those DNA strands with a Cas9 endonuclease, allowing for genes to either be removed or

added[6,11]. The CRISPR/Cas9 system offers the most efficient method to target specific DNA sequences in human cells; that system, combined with stem cells, further advances the potential of autologous cell therapies by allowing us to genetically correct disease phenotypes in patient-specific hiPSCs and derivatives. Recent studies have demonstrated successful CRISPR/Cas9-mediated correction of hiPSC-derived neural cells, muscle cells, and hepatocyte cells[8,12,13].

Despite the potential of hiPSCs to revolutionize biomedical research and medicine, there are still numerous obstacles, such as genomic instability, immunogenicity, and tumorigenicity of hiPSCs, which raise questions concerning the safety of hiPSCs for autologous cell transplants. Genomic instability is a common occurrence in pluripotent stem cells, having first been observed in human embryonic stem cell (hESC) lines. Common genomic abnormalities that have been observed in hiPSCs and hESCs include development of chromosomal aneuploidies, copy number variations (CNV), loss of heterozygosity (LOH), and gene deletions[14,15]. Although the impact that genomic instability of hiPSCs has on safety for autologous cell transplantations is debated, certain mutations are potentially tumorigenic, therefore negating any beneficial clinical purpose that they may serve.

In the following studies, we aim to address two areas of need in the stem cell field: first, to investigate the causes of genomic instability in hiPSCs, and second, to develop methods to efficiently and safely modify hiPSCs to correct for single enzyme disorders. The results of these studies will hopefully contribute to the advancement of stem cell research to clinical applications.

Chapter 1: Nucleoside supplementation restores dNTP balance and alleviates genomic instability in hiPSCs

Introduction

There are three conditions under which hiPSCs can acquire mutations: from pre-existing mutations in the parental cells, through the reprogramming, and during long-term *in-vitro* culture[14,15,16]. Commonly used protocols for reprogramming human somatic cells into hiPSCs require the "Yamanaka factors," which include the oncogenes *cMyc* and *Klf4*. Oncogenes have been shown to induce genomic instability in cancer cell lines via elevating levels of DNA replication stress and damage, use of *cMyc* and *Klf4* in the reprogramming process potentially promotes genomic aberrations such as CNVs in hiPSCs post-reprogramming[17]. Additionally, culture-mediated selection pressures that lead to genomic instability in hiPSCs are not attributable to one factor alone; rather, the instability is a result of various independent or a combination of factors. Potential culture stresses that may affect the genomic stability of hiPSCs include: oxygen tension, mechanical versus enzymatic passaging, basement membrane matrix, and media components such as growth factors[18]. After reprogramming human somatic cells into hiPSCs, the cell cycle profile of stem cells is dramatically altered. Unlike differentiated cells, which spend around 40% of the cell cycle in G1 phase, hiPSCs and hESCs have a shortened cell cycle, spending approximately 15% of their in G1 and 65% in S phase[19,20,21]. The shortened cell cycle maintains the self-renewal capabilities of pluripotent stem cells, which regulates pluripotency downstream[19]. Therefore, due to the accelerated cell cycle in hiPSCs, the cellular DNA replication machinery may encounter

issues in balancing successive rounds of replication and DNA damage repair at high fidelity, leading to an increase of double-stranded DNA breaks (DSBs). Additionally, given that the endogenous replication machinery of hiPSCs has to account for the accelerated rounds of DNA replication, hiPSCs may have a higher sensitivity to exogenous pressures from culture adaptation.

The current focus on genomic instability in stem cells is on both detection and prophylactic solutions. Basic detection methods include karyotype analysis and fluorescence in situ hybridization (FISH), both of which reveal chromosomal number and structural changes in hiPSCs[22]. Karyotype analysis and FISH are useful to detect the presence of both inter-chromosomal rearrangements and gains and losses of chromosomes. In order to detect subchromosomal alterations such as point mutations and deletions, higher resolution methods are necessary. Comparative genomic hybridization (CGH) and single nucleotide polymorphism (SNP) arrays directly measure DNA content and are able to detect changes on the exon level[23]. These high-resolution methods can be used to detect changes in CNVs and LOH as well as changes in gene expression in hiPSCs after reprogramming and long-term culture. However sequencing methods, despite increased sensitivity, are expensive and require extensive time to draw conclusions from the data. Even though characterization of genomic aberrations is vital to understanding genomic instability in hiPSCs, given the genomic heterogeneity of a hiPSC population at any given point in culture, it would be difficult to target any one specific mutation. Recently, emerging research has turned to media supplementation to alleviate levels of DNA damage in hiPSCs while in culture. While small molecules are commonly used in stem cell culture to prevent apoptosis or enhance cell growth, two

recent and independent studies have supplemented culture medium with antioxidants during reprogramming and culture[24,25]. hiPSCs grown in antioxidant-supplemented media had lower levels of DSB markers γH2AX and 53BP1, suggesting a protective effect from reactive oxygen species (ROS) that are elevated during reprogramming and culture[26]. However, despite a decrease in CNVs and DNA damage with antioxidant supplementation, other genomic abnormalities such as point mutations still occur, suggesting that there are multiple sources of genomic instability in hiPSCs.

The goal of this first aim is to investigate the role of replication-stress induced nucleotide deficiency on promoting genomic instability in hiPSCs and the use of nucleoside supplementation to alleviate DNA damage in stem cells. Since cell cycle is accelerated and DNA damage checkpoints are altered post-reprogramming in hiPSCs compared to parental fibroblasts, it is conceivable that replication stress plays a role in heightened DNA damage in the stem cells. In cancer cells, chromosomal abnormalities are attributed to replication stress-induced DNA damage and an insufficient pool of nucleotides to support normal replication and maintenance of genomic integrity[27]. Supplementation of a defined nucleoside cocktail rescues endogenous nucleotide pools in cancer cells, leading to decreased DNA damage and increased genomic stability. Additionally, it has recently been demonstrated that supplementation with a commercially available ribonucleoside cocktail can alleviate DNA damage during reprogramming[28]. It has, however, not been reported if stem cells also have lower endogenous nucleotide pools as a result of altered cell cycle kinetics and if supplementation with nucleosides can alleviate DNA damage during *in-vitro* culture. We demonstrate that reprogramming somatic cells into hiPSCs causes a reduction of

endogenous deoxynucleotide (dNTP) pools, which are essential for maintaining DNA replication and repair. The decline in dNTP pools potentially contributes to the heightened incidence of DNA double-stranded breaks (DSBs) due to replication stress in hiPSCs. Furthermore, supplementation of culture media with a defined cocktail of four deoxyribonucleosides (dNs) significantly recovers endogenous dNTP pools and reduces incidence of DSBs in hiPSCs, indicating a potential tool to prevent genomic instability in stem cells.

Materials and Methods

hiPSC and dermal fibroblast cell culture

xcHUF1, mRNA-BJ, and AD1 hiPSCs were grown in feeder-free conditions consisting of reduced growth factor Matrigel (BD Biosciences, San Jose, CA) and a 50:50 mix of mTeSR1 media (StemCell Technologies, Vancouver, BC, Canada) and Nutristem (Stemgent, San Diego, CA) supplemented with 1x Primocin (InvivoGen, San Diego, CA) and 10 mm bFGF (Biopioneer, San Diego, CA). Cells were passaged every 4 days using a disposable STEMPRO EZ passage tool (Thermo Fisher, Waltham, MA) by cross-hatching uniform pieces and transfering to a freshly-coated Matrigel plate. For putative clinical-grade conditions, CELLstart (Thermo Fisher) was used in place of Matrigel and prepared per manufacturer's instructions. Clinical-grade hiPSCs were cultured in xeno-free Nutristem supplemented with 1x Primocin and 10 mM bFGF. All procedures were approved by the Institutional Review Board (IRB #13-001469-AM-00002) and the Embryonic Stem Cell Research Oversight (ESCRO) (ESCRO #2010-

010-04A) Committee of the University of California, Los Angeles and informed consent was documented from patients.

Dermal fibroblasts were cultured in complete DMEM/F-12 media comprised of DMEM nutrient mixture/F-12, 10% fetal bovine serum (FBS), 1x minimum essential medium non essential amino acid, 1x Glutamax, and 100 IU/ml penicillin-streptomycin (all from Invitrogen, Grand Island, NY). Fibroblasts were passaged with 0.05% trypsin-ethylenediamine tetraacetic acid (Invitrogen).

Deoxyribonucleoside supplement formulation

Deoxyribonucleoside supplement was prepared by resuspending 2'-deoxycytidine and thymidine (Sigma-Aldrich, St. Louis, MO) in water and 2'-deoxyadenosine monohydrate and 2'-deoxyguanosine monohydrate (Sigma-Aldrich) in DMSO. Stock solutions were stored in -80°C. Stock nucleoside solutions were further diluted in aliquots of culture media and stored at -80°C. Each day, these stocks were thawed and added to pre-warmed culture medium to reach final appropriate concentrations before adding to cell cultures. For the candidate dN cocktails, the concentrations tested were: A (30 μM dC, 30 μM dA, 30 μM dT, 30 μM dG); B (30 μM dC, 30 μM dA, 5 μM dT, 5 μM dG); C (30 μM dC, 5 μM dA, 5 μM dT, 5 μM dG); D (5 μM dC, 5 μM dA, 5 μM dT, 5 μM dG); and E (5 μM dC, 1 μM dA, 1 μM dT, 1 μM dG).

γH2AX immunofluorescence

hiPSCs were plated on Matrigel-coated 12mm circular glass coverslips (Neuvitro, Braunschweig, Germany). Cells were washed in 1x PBS and fixed with 4%

paraformaldehyde (Polysciences, Warrington, PA). Samples were permeabilized in 1% Triton X-100 (Sigma-Aldrich) for 1 hour at room temperature then blocked with 5% goat serum (Sigma-Aldrich) in PBS for 1 hour at room temperature. Primary γH2AX antibody (Cell Signaling Technology, Danvers, MA) was diluted 1:400 in blocking buffer and incubated overnight at 4°C. After primary incubation, cells were washed 3x for 5 minutes each with PBS. Goat anti-Mouse IgM Alexa Fluor 488 (Life Technologies, Carlsbad, CA) was diluted 1:500 in blocking buffer and incubated for 45 minutes at room temperature. After secondary antibody incubation, cells were washed 3x for 5 minutes each with PBS, and incubated with 1x DAPI (Thermo Fisher) for 7 minutes followed by 2x 3 minute PBS washes. Coverslips were mounted on slides and fluorescence images were captured and processed with an Axiocam MR Monocolor Camera and Axiovision Digital Image Processing Software (Carl Zeiss, Jena, Germany).

γH2AX foci quantification

Images of the samples were taken in a blinded manner to avoid bias. For data collection, 50 nuclei per sample were counted and images were blind quantitated by three different people. Only nuclei that contained 3 or more foci were considered damaged, and nuclei that had high fluorescence but no distinct foci were considered apoptotic and therefore not included in the final analysis.

dNTP enzymatic assay

The protocol was adapted from Mathews et al., 2009. Cells were plated and cultured for 4 days to 60% confluency. Cells were harvested and $1x10^6$ cells were

collected, washed with cold PBS, and centrifuged at 80 g for 10 minutes. The supernatant was then aspirated, and the pellet resuspended in 60% methanol and vortexed on high for 1 minute. The suspension was placed at -20°C overnight. Samples are then boiled for 2 minutes, placed on ice for 15 minutes, then centrifuged at 1,200 g for 10 minutes. The supernatant was collected and transferred to new tubes and centrifuged again at 17,000 g for 10 minutes. The resulting supernatant was transferred to new microcentrifuge tubes (Sigma-Aldrich) with pre-punctured holes on top and the extract dried for 8 hours using a Speed-Vac (Thermo Scientific). The extract was resuspended in 100 ml of nuclease free water.

For the enzymatic assay, a master mix was prepared with 10x Buffer 2 (New England BioLabs, Ipswich, MA), nuclease free water, 50 mM oligonucleotide template, Klenow Fragment DNA polymerase (New England BioLabs), and [^{3}H]dTTP (Moravek Biochemicals, Brea, CA). Sequences for the oligonucleotide templates for dCTP, dTTP, dATP, and dGTP used are detailed in Mathews et al., 2009. 20 ml of master mix and 5 ml of the sample extract were mixed into a 96-well V-bottom plate (Thermo Fisher) and centrifuged to mix samples. Reactions were incubated at 37°C for 2 hours to allow reactions to go to completion. 15 ml of each reaction was spotted on a 15 mm Whatman filter paper (Sigma Aldrich), placed in a scintillation vial and fluid, and measured in a Beckman Model LS 6500 Scintillation Counter System (Beckman Coulter, Brea, CA). All experiments were performed in triplicate.

hiPSC growth rate calculation

Areas of hiPSC colonies were measured and tracked using the Axiovision Digital Image Processing Software (Carl Zeiss) and recorded daily. Growth rate was measured by compiling colony growth ratios, calculated by dividing the area of a hiPSC colony with the area of the previous day. Growth rates for individual dNs and triple dN supplements were normalized to the initial day. For the final candidate dN growth rate measurements, we measured colony areas at 24 and 48 hours and calculated growth ratios.

Karyotype analysis

hiPSCs were cultured to 95% confluency in 25 cm^2 flasks and delivered for G-band karyotyping analysis (Cell Line Genetics, Madison WI).

Statistical Analysis

All collected data was analyzed with the SPSS (Armonk, NY) statistical package (Version 21.0). Results were expressed as mean ± standard deviation (SD) and p-values were determined using an unpaired two-tailed t-test to examine significance between comparisons. Error bars represent SD.

Results

hiPSCs have lower dNTP pools and elevated incidence of DNA damage

Recent studies have demonstrated that hiPSCs undergo significant replication stress (RS) during reprogramming and cell culture and are highly susceptible to DNA damage-induced apoptosis[15,16,28,29]. RS is a form of DNA damage that is caused by

misregulation of ataxia telangiectasia and Rad3-related (ATR) and checkpoint kinase 1 (CHK1) kinases and stalled replication forks[28]. The destabilization of replication forks caused by insufficient dNTP pools can lead to DSBs. Overexpression of CHK1, a key serine/threonine kinase required for checkpoint-mediated cell cycle arrest and activation of DNA damage repair mechanisms, can reduce reprogramming-induced replication stress on hiPSCs[30,31]. To measure incidence of DNA damage, we analyzed the levels of H2AX phosphorylation (γH2AX), a marker of DSBs, in hiPSCs, derived in our lab, and compared those levels to their parental dermal fibroblasts. Specifically, we included two lines derived with an integrating lentiviral cassette (xcHUF1 and AD1) and one line derived via non-integrating mRNA transfection (mRNA-BJ). Both reprogramming methodologies delivered the *Oct4*, *Sox2*, *Klf4* genes and the oncogene *cMyc*. To compare incidence of DSBs between hiPSCs and fibroblasts, we performed immunocytochemistry for γH2AX and quantified the number of damaged nuclei (determined as ≥3 γH2AX foci per nuclei) among a population of 50 blinded cells. Compared to parental dermal fibroblasts, xcHUF1, mRNA-BJ, and AD1 hiPSCs all demonstrated a higher number of γH2AX-positive nuclei per 50 cells (Figure 1-1). These data suggests that hiPSCs, regardless of reprogramming method, have higher incidence of endogenous DNA damage compared to their parental somatic cells post-reprogramming.

While the causes of RS are not clearly understood, RS has been linked to insufficient levels of endogenous deoxynucleotides needed to maintain proper DNA replication and repair in cancer cell lines[27,32,33]. Due to similarities between stem cells and cancer cells, namely the ability to self-renew and form teratomas, we measured

levels of endogenous deoxynucelotide (dNTP) pools in hiPSCs and parental dermal fibroblasts. A enzymatic assay, designed to quantify endogenous cellular dNTP levels, revealed that xcHUF1, mRNA-BJ, and AD1 hiPSC lines had significantly lower levels of deoxycytidine triphosphate (dCTP), thymidine triphosphate (dTTP), deoxyadenosine triphosphate (dATP), and deoxyguanosine triphosphate (dGTP) compared to parental dermal fibroblasts (Figure 1-2). Notably, the lower pools and higher incidence of DSBs in the mRNA-BJ line demonstrate that, though integration and residual exogenous expression of the oncogene *cMyc* may play a role in RS in the xcHUF1 and AD1 lines, decreased levels of dNTP pools may be an inherent characteristic of hiPSCs regardless of reprogramming methology and may play a significant role in observed genomic instability.

Candidate deoxyribonucleoside supplements do not cause significant long-term toxicity to hiPSCs

Mammalian cells maintain and synthesize a proper balance of dNTPs by using either the de novo pathway (DNP) or the nucleotide salvage pathway (NSP)[34]. The NSP produces dNTPs by recycling degraded bases and nucleosides from the extracellular environment and converting them back into nucleotides for DNA synthesis. Recent studies have demonstrated that by supplementing culture media with exogenous ribonucleosides, stem cells can utilize their cellular NSP both to increase proliferation rates as well as to alleviate DNA damage and copy number variations (CNVs)[31,35]. Therefore, as conventional hiPSC culture media does not contain nucleotides for NSP use, we sought to develop and optimize a deoxyribonucleoside-based supplement (dN)

in order to investigate and further enhance its effect on restoring dNTP pools and alleviating DNA damage in hiPSCs. First, we measured toxicity of individual dNs on xcHUF1 hiPSCs by culturing the cells over 2 passages in 5 different conditions: vehicle, 30 μM deoxycytidine (dC), 30 μM thymidine, 30 μM deoxyguanosine (dG), or 30 μM deoxyadenosine (dA). After 8 days of dN supplementation, hiPSC colony growth rate decline compared to the vehicle control. Notably, supplementation of 30 μM dT and dG led to the most significant short-term toxicity (Figure 1-3); high concentrations of dT can interrupt the dNTP metabolism pathway and arrest cells in S-phase. Since all four dNs are required to maintain balanced dNTP pools, but not necessarily in equimolar concentrations, we aimed to optimize the final cocktail composition by culturing hiPSCs with different combinations comprised of equimolar concentrations of three dNs over 8 days. Cells that were treated with a supplement condition without dC had an average growth rate that was around 2x slower than the control and other conditions (Figure 1-3). Furthermore, the vehicle condition maintained the highest growth rate, suggesting that an equimolar concentration of all 4 dNs were not optimal.

With the data gathered from the short-term growth rate and toxicity experiments, we tested 5 supplement conditions, each containing varying concentrations of each of the 4 dNs, over a long-term period of 30 days. Using the toxicity data from the individual and triple dN experiments, we created 5 supplements that contained a greater concentration of dC and dA and lowered concentrations of dT and dG to minimize long term toxicity but still exogenously supply all four dNs. Measurements recorded at 24 hours, 4 days, and 30 days showed no significant long-term day-to-day toxicity in any of our supplement conditions compared to the vehicle control (Figure 1-

4). Supplement B (30 μM dC, 30 μM dA, 5 μM dT, 5 μM dG) increased xcHUF1 hiPSC growth rate compared to vehicle at the end of 30 days; furthermore, hiPSCs cultured with dN supplement B showed the greatest decrease in γH2AX-positive nuclei in xcHUF1 hiPSCs, reducing incidence by ~30%, $p < 0.0001$ (Figure 1-6). Therefore, we selected supplement B as the primary candidate for subsequent experimental studies.

Deoxyribonucleoside supplementation recovers dNTP pools and alleviates DNA damage in hiPSCs

After optimization of our nucleoside cocktail in xcHUF1 hiPSCs, we expanded our investigation of its effect on dNTP pools and DNA damage to include mRNA-BJ and AD1 hiPSCs. After two weeks of culture, hiPSCs cultured with supplement B exhibited a recovery of endogenous levels of dCTP, dTTP, dATP, and dGTP levels (Figure 1-5). dN supplement B also significantly reduced incidence of DSBs in mRNA-BJ and AD1 hiPSCs after a two week treatment compared to vehicle, demonstrating the supplement's applicability and efficaciousness across multiple independently-derived lines (Figure 1-7). Use of our dN supplement also resulted in a greater reduction γH2AX-positive nuclei in hiPSCs compared to a ribonucleoside supplement, suggesting that dNs provide a greater effectiveness in preventing RS-induced genomic instability (data not shown).

Lastly, as one of the goals of stem cell research is to translate the technology to clinical applications, it is essential to convert hiPSCs to xeno-free clinical-grade culture conditions[36]. However, this conversion process induces a considerable amount of strain and selective pressure on hiPSCs, which increases the chance of developing significant

genomic alterations. Supplementation of exogenous ribonucleosides reduces the number of CNVs in hiPSCs and prevents aneuploidy in cancer lines[31,37]. Therefore, we investigated if supplementation of hiPSCs with dNs could prevent the sporadic development of aneuploidy. We tested vehicle and supplement B conditions, with three subclones per condition, and observed that after two months of culture and conversion to clinical-grade conditions, all lines maintained normal karyotype. However, all three unsupplemented hiPSCs showed signs of non-clonal chromosomal aberrations (NCCAs), while only one supplemented line exhibited any NCCAs (Figure 1-8). Until recently, NCCAs have been regarded as genetic "noise;" however, additional research is interpreted to suggest that they may play a larger role in cellular heterogeneity and cellular adaptation to stress[38]. Therefore, since detecting aneuploidy is not a sufficient metric to investigate the effect of nucleoside supplementation on preventing stress-induced genomic damage, further studies are needed to measure changes in small-scale genomic alterations.

Discussion

In this study, we 1) identified an imbalance of dNTP pools as a key contributor to genomic instability in hiPSCs and 2) developed a novel deoxyribonucleoside-based supplement that could be used to treat hiPSC lines to augment dNTP pools and alleviate endogenous DNA damage. While the reason for lowered dNTP pools in hiPSCs still needs to be elucidated, it is evident from our data that RS-induced DNA damage could be a result of altered cell cycle kinetics and lowered nucleotide pools, leading to an insufficient supply of dNTPs to maintain DNA replication and repair.

Furthermore, by augmenting endogenous dNTP pools utilizing the hiPSCs' nucleoside salvage pathway, we can reduce incidence of DNA damage, and potentially the development of long-term genomic instability in culture.

Genomic instability in hiPSCs is a complex issue that is not well understood and can have severe implications in the translation of the technology to therapeutic applications. Our study focuses on only one possible avenue to explore by investigating the role of endogenous nucleotide pools in RS-induced DNA damage in hiPSCs and provides a safe, universally applicable solution that can be used to aid in preventing genomic instability. Further investigation is needed to test the effect of our dN supplement on reprogramming and differentiating hiPSCs. RS decreases reprogramming efficiency and both overexpression of CHK1 and supplementation with ribonucleosides can counterbalance the effects of RS[31]. Since we have demonstrated that deoxyribonucleosides are more effective than ribonucleosides in alleviating DNA damage *in vitro*, if dNs can further increase reprogramming or differentiation efficiency, our studies would provide a universally-applicable culture-based tool that can prevent genomic instability in hiPSCs without genetically modifying any hiPSC lines.

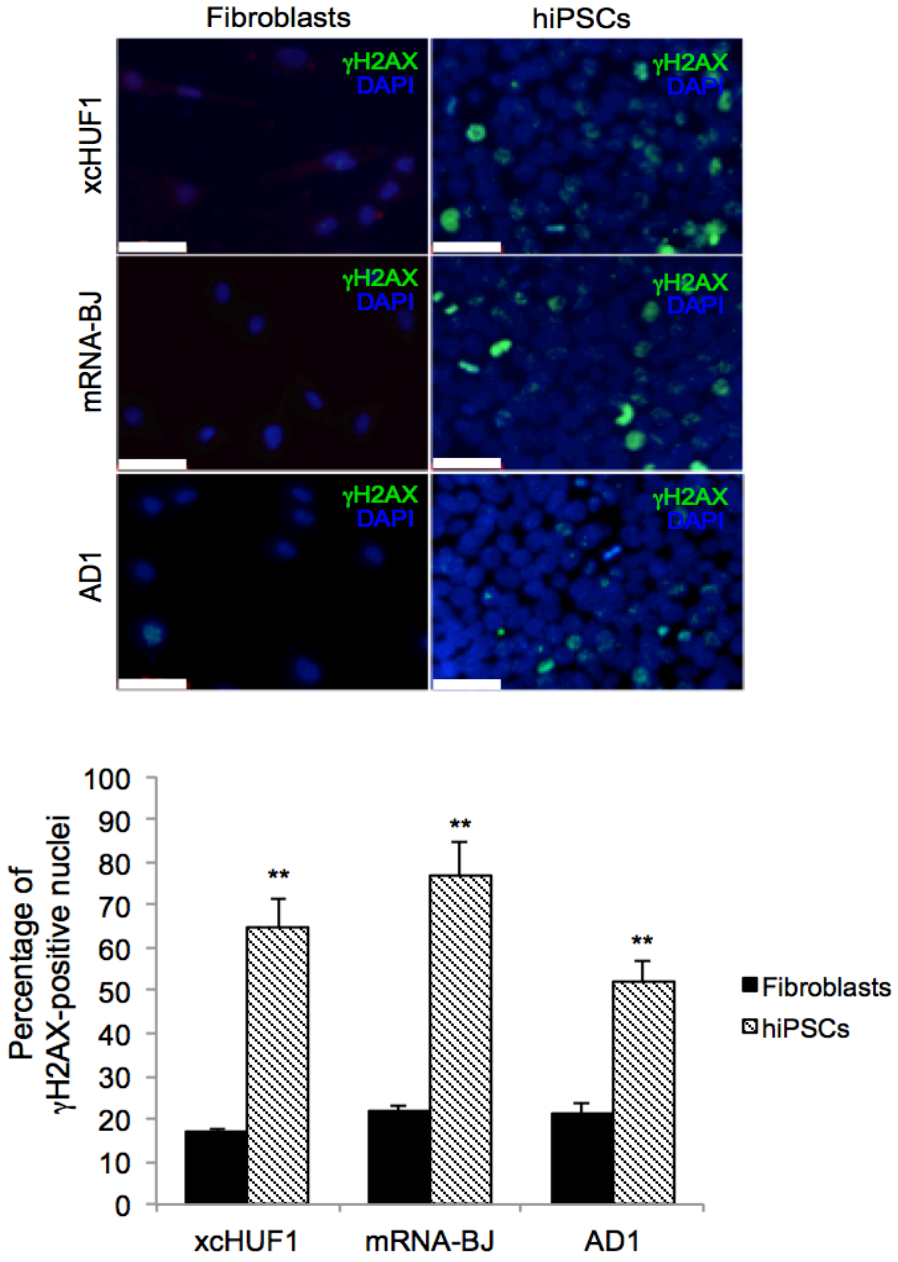

Figure 1-1 γH2AX expression and dNTP levels in xcHUF1, mRNA-BJ, and AD1 hiPSCs

(A) Visual comparison and quantification of γH2AX-positive nuclei in xcHUF1, mRNA-BJ, and AD1 hiPSCs (n=50). γH2AX foci were detected via immunofluorescence and three blind counts were performed to eliminate bias. Data are represented as means ± SD. **p<0.05 unpaired two-tailed t-test.

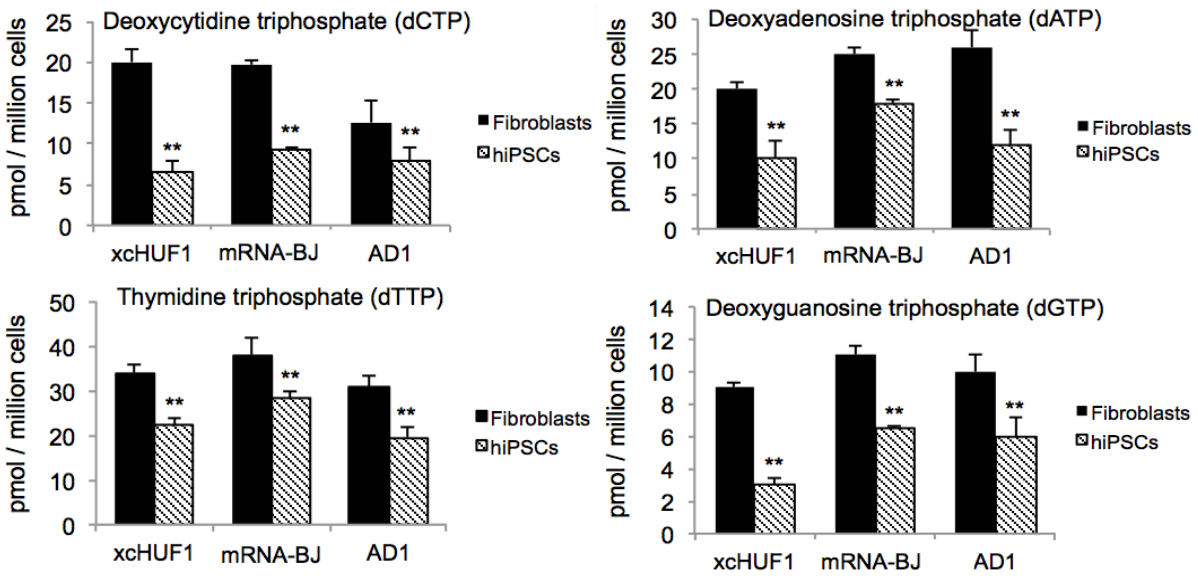

Figure 1-2. dNTP levels in dermal fibroblasts and hiPSCs

Quantification of endogenous deoxycytidine triphosphate (dCTP), thymidine triphosphate (dTTP), deoxyadenosine triphosphate (dATP), and deoxyguanosine triphosphate (dGTP) in xcHUF1, mRNA-BJ, and AD1 hiPSC and fibroblasts (n=9). Data are represented as means ± SD. **p<0.05 unpaired two-tailed test..

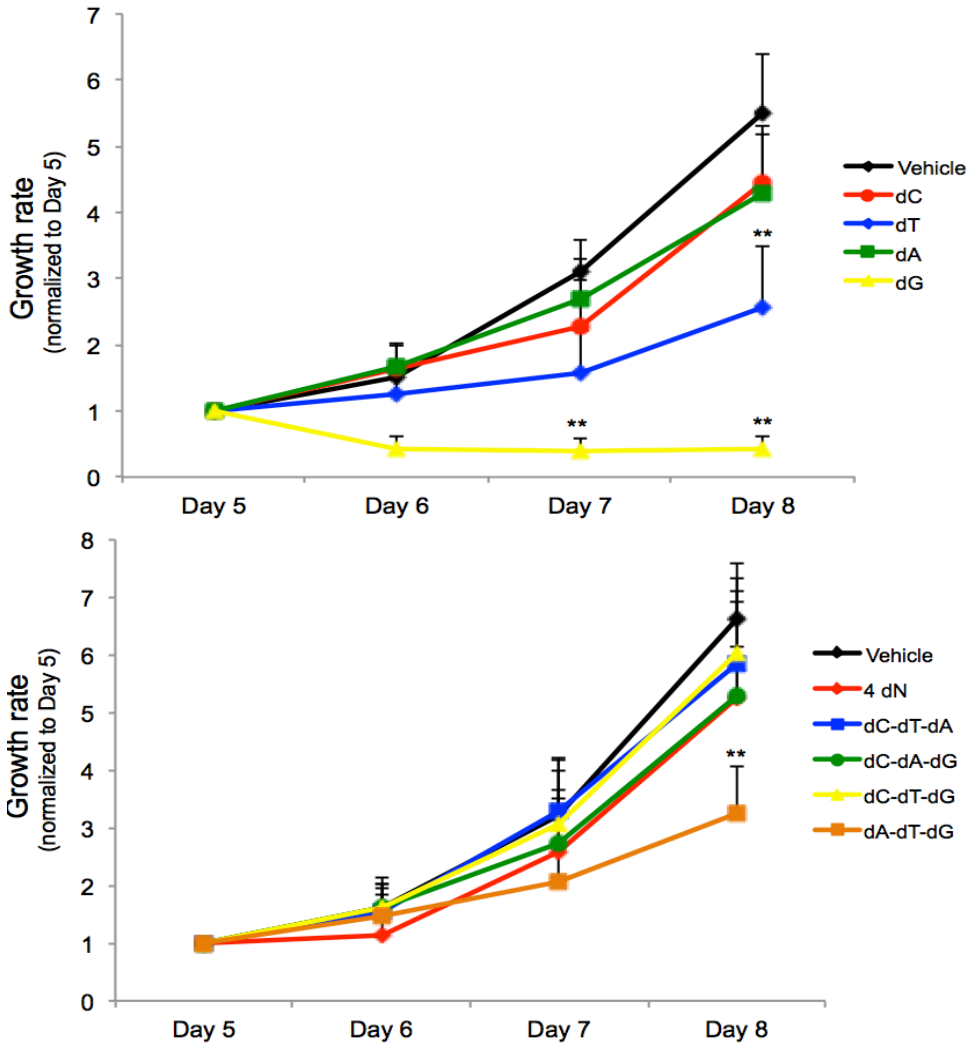

Figure 1-3. Optimization of deoxyribonucleoside supplement

(Top) Growth rate of xcHUF1 hiPSCs cultured in individual dN conditions for 8 days (2 passages). Areas of hiPSC colonies (n=20) were normalized to day 5 and growth rates are represented by the ratio of colony areas. Data are represented as means ± SD. **p<0.05 unpaired two-tailed t-test compared to the colony area size in day 5. **(Bottom)** Growth rate of xcHUF1 hiPSCs grown with different equimolar (30 mM) combinations of three dNs for 8 days (2 passages). Areas of hiPSC colonies (n=20) were normalized to day 5 and growth rates were calculated as ratios of areas. Data are represented as means ± SD. **p<0.05 unpaired two-tailed t-test compared to the colony area size in day 5.

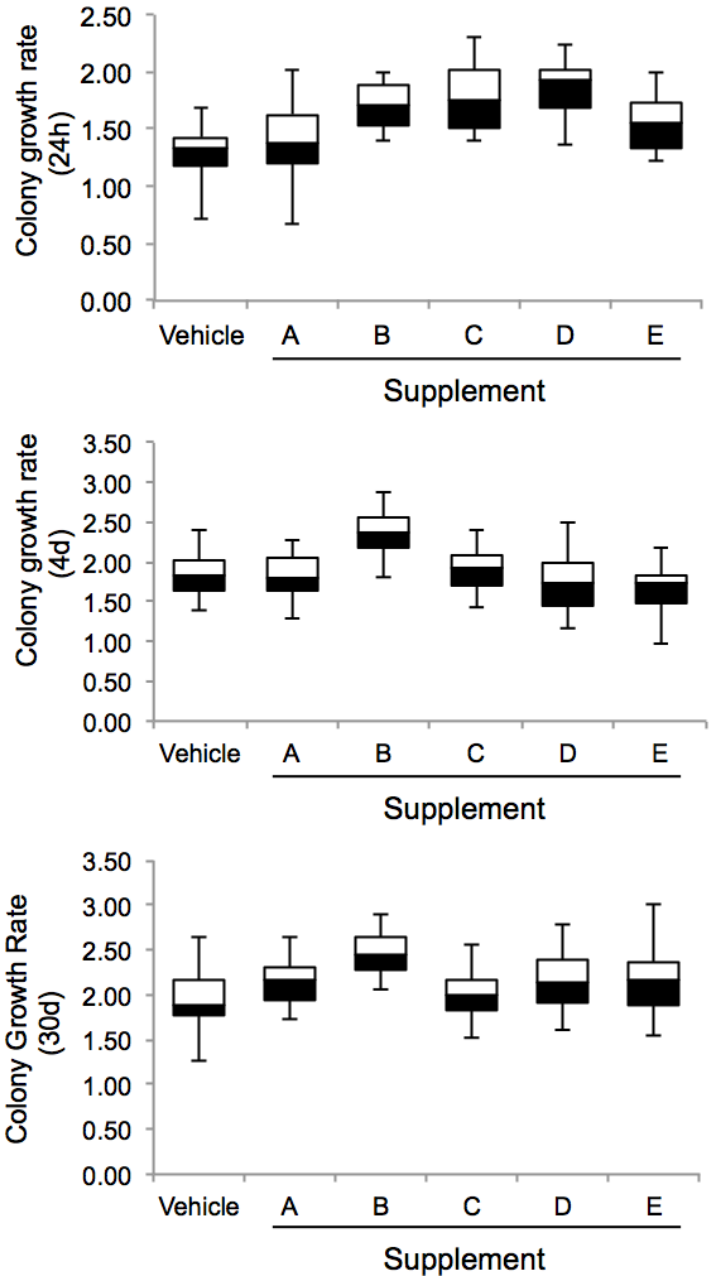

Figure 1-4. hiPSC growth rates with 5 candidate dN supplements

Growth rates of xcHUF1 hiPSCs (n=20) cultured with one of five candidate dN supplement conditions are represented in boxplots. Boxes show the median, 25th, and 75th percentiles, error bars represent the 10th and 90th percentiles. Measurements were taken 48 hours post-plating and were normalized to the colony area 24 hours post-plating.

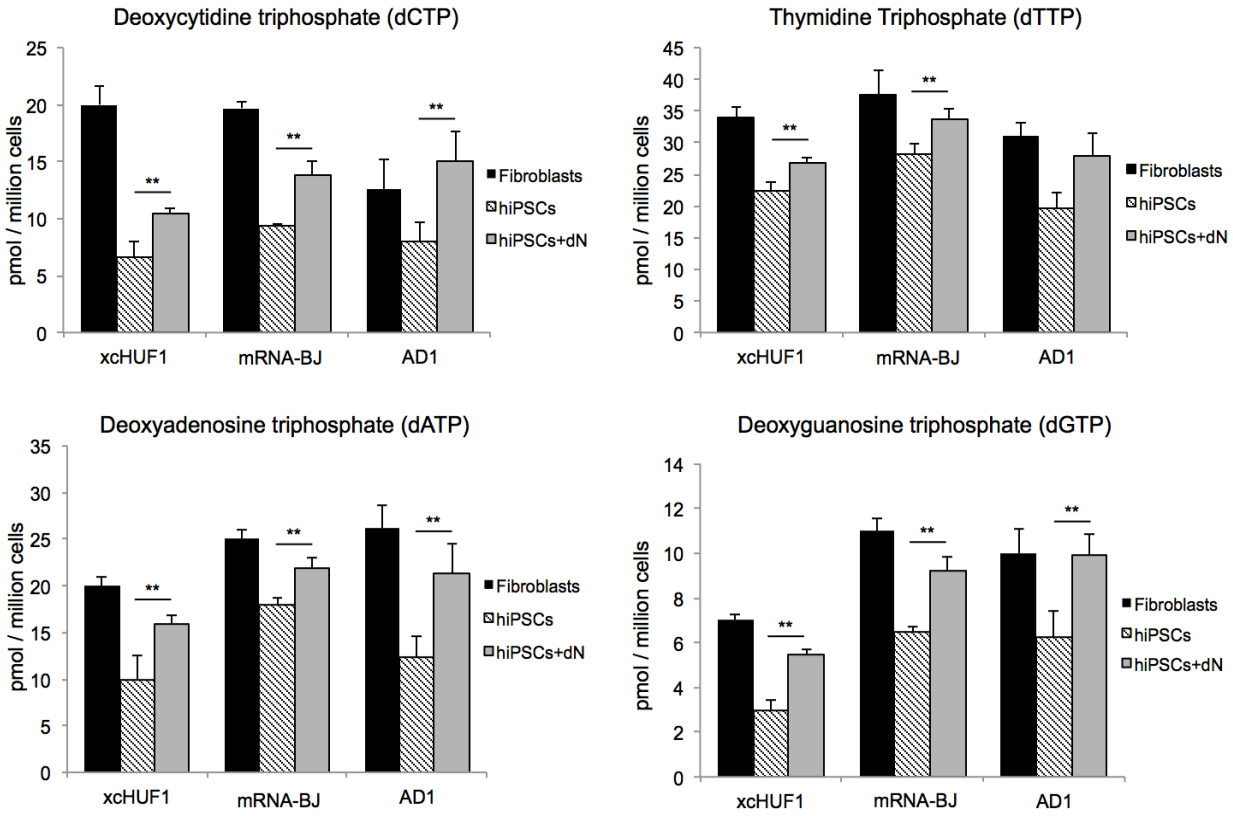

Figure 1-5. Recovery of dNTP pools with deoxyribonucleoside supplementation

Quantification of dNTP pools in hiPSCs after two weeks of daily supplementation with deoxyribonucleosides and comparison to parental fibroblasts and unsupplemented hiPSCs (n=9). Data are represented as means ± SD. **p<0.05 unpaired two-tailed test.

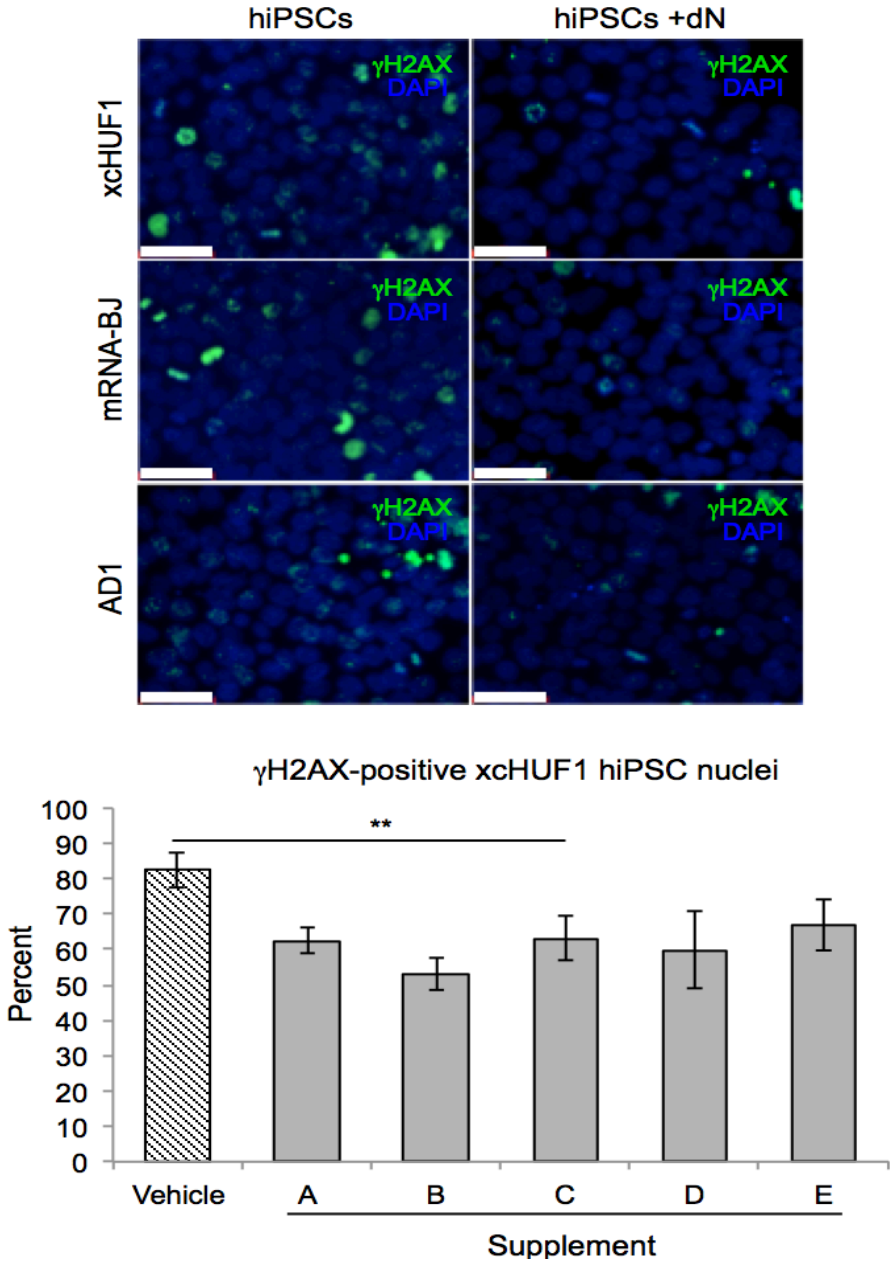

Figure 1-6. dN supplementation lowers levels of γH2AX in xcHUF1 hiPSCs

(Top) Immunofluorescence of γH2AX foci in unsupplemented and supplemented hiPSCs. hiPSCs for both conditions were cultured simultaneously and the supplemented condition was treated daily. **(Bottom)** Quantification and comparison of γH2AX-positive nuclei for xcHUF1 hiPSCs (n=50) across 5 different supplement formulations. Samples were stained after 30 days and nuclei were counted by three independent blinded tests. Data are represented as means ± SD. **p<0.05 unpaired two-tailed t-test and compared to vehicle.

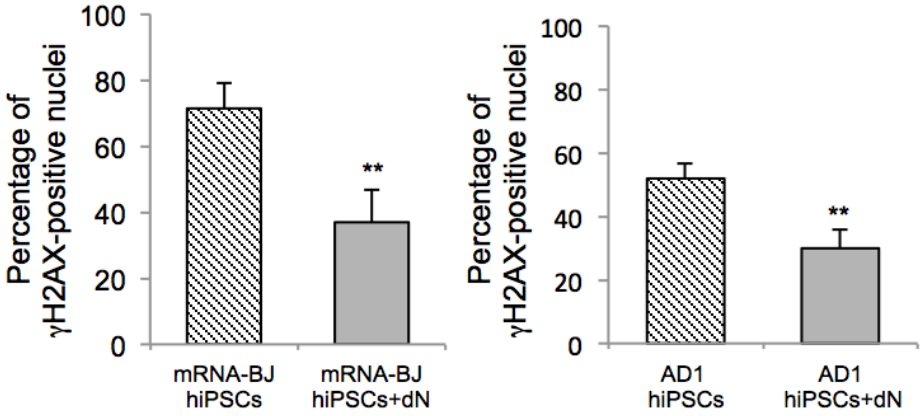

Figure 1-7. Supplementation lowers γH2AX levels in mRNA-BJ and AD1 hiPSCs

Quantification of gH2AX-positive nuclei in mRNA-BJ and AD1 hiPSCs after a two-week treatment with dN Supplement B. Three blind counts were performed to quantify nuclei. Data are represented as means ± SD. **p<0.05 unpaired two-tailed t-test.

Unsupplemented hiPSC	Karyotype	Non-clonal chromosomal aberrations
Subclone 1	46,XX	1. 45,XX, -14 2. 45, XX, -17
Subclone 2	46,XX	1. 45,XX, -16 2. 45, XX, -12
Subclone 3	46,XX	1. 45,XX, -13

Supplemented hiPSC	Karyotype	Non-clonal chromosomal aberrations
Subclone 1	46,XX	None
Subclone 2	46,XX	None
Subclone 3	46,XX	1. 45,XX, -17 2. 45, XX -13

Figure 1-8. dN supplementation reduces NCCAs in hiPSCs after conversion to putative clinical-grade culture conditions

Karyotype analysis of xcHUF1 hiPSCs after conversion to putative clinical-grade culture conditions with or without dN supplement. Three subclones of each condition were analyzed.

Chapter 2: Restoring ureagenesis in hepatocytes by CRISPR/Cas9-mediated genomic addition to arginase-deficient induced pluripotent stem cells

Introduction

Urea cycle disorders (UCDs) are rare enzymopathies with an incidence of 1:35,000 births resulting in approximately 113 new cases per year in the United States[39]. They are a significant cause of inherited hyperammonemia and afflicted infants and newborns are at substantial risk of recurrent brain injury and death. Excessive plasma ammonia is neurotoxic, resulting in central nervous system injury including intellectual disabilities, seizures, loss of psychomotor function with continued nitrogen vulnerability[39,40,41,42,43]. UCDs result from a deficiency in one of six hepatic enzymes and two mitochondrial transporters that regulate nitrogen metabolism and urea production and are typically classified as an inborn errors of metabolism[39,40,41,43].

Hyperargininemia, or arginase deficiency, is an autosomal recessive disorder that affects the final step of the urea cycle. Patients who exhibit hyperargininemia typically present after the neonatal period with spasticity, seizures, spastic diplegia, and developmental regression, differing from the other urea cycle disorders[40,44,45,46]. Arginase 1 (*Arg1*) is primarily located in the liver, hydrolyzing arginine to urea while regenerating ornithine to continue the cycle[45,46]. Loss of *Arg1* activity results in an inability to remove nitrogen from arginine, but rarely causes symptoms of hyperammonemia. Instead, the cause of the pathogenesis of neurological deterioration in arginase deficiency is not known and is thought to be due to unique biochemical abnormalities such as elevated guanidino compounds, nitric oxide, or glutamine[43,46,47,48].

As there is no completely effective treatment for urea cycle disorders, the mainstay of therapy is dietary protein restriction, with emergency treatments for hyperammonemia consisting of dialysis, hemofiltration and intravenous administration of nitrogen scavenging drugs[40]. Chronic therapy is minimally effective in reducing plasma ammonia while control of hyperargininemia may delay the onset of symptoms but may not ultimately prevent the progressive and relentless nature of neurocognitive decline[44,46]. Liver transplantation is the extreme alternative to conventional therapies to prevent progression of neurological injury in UCD patients. However, the demand for liver donors far exceeds the supply, and other avenues, such as genetic modification and cell replacement therapy, need to be explored to treat these disorders.

Since the demonstration that human induced pluripotent stem cells (hiPSCs) could be reprogrammed from fibroblasts with four transcription factors (*Oct4*, *Sox2*, *Klf4*, and *cMyc*), hiPSCs have emerged as a potential avenue for patient-specific disease modeling and development of therapy[49,50,51,52,53]. Whereas the difficulty in obtaining primary cell cultures previously hindered progress of disease research, the ability of patient-specific hiPSCs to differentiate into genetically similar somatic cell types of various lineages, such as hepatocytes, allows for the generation of a substantial quantity of patient-specific cells[54,55]. These hiPSC-derived hepatocytes express liver-specific markers such as albumin (*ALB*), alpha-fetoprotein (*AFP*), and cytokeratin 18 (*CK18*) as well as functionality markers such a1-antitrypsin (*AAT*) and *CYP3A4*, demonstrating their phenotypic similarity to endogenously derived hepatocytes[55]. Reprogramming patient-specific hiPSCs and establishing isogenic and functional derivatives afford the advantage of avoiding the ethical controversy of oocyte-derived

embryonic stem cell use and potentially addressing the immunogenicity issues for cell replacement therapies[56].

In this study, we sought to correct the enzyme deficiency, using a universal approach, in multiple arginase-deficient hiPSC lines derived from hyperargininemic patients by using genome editing technology. We delivered CRISPR/Cas9 nickases via nucleofection for gene addition of a full-length codon-optimized human arginase 1 cDNA (ArgO) expression cassette (LEAPR) into Exon 1 of the endogenous hypoxanthine-guanine phosphoribosyltransferase (*HPRT*) locus in hiPSCs[6]. After targeted insertion and puromycin selection (enabled by the LEAPR-derived puromycin N-acetyl-transferase [PAC]), and with confirmation of the presence of the LEAPR cassette in the patient-specific hiPSCs, we demonstrated the restoration of arginase activity in both hiPSCs and differentiated hepatocyte-like cells. Results from this genetic targeting approach potentially offer a widely applicable method to genetically introduce arginase expression in hiPSCs derived from hyperargininemic patients and, on a broader scale, to other single-enzyme inborn errors of metabolism.

Materials and Methods

In vitro derivation and culture of primary human dermal cells

The control human dermal fibroblast cell line (xc-HUF1), obtained from UCLA Good Manufacturing Practice (GMP) facility, and two disease fibroblast lines (AD2 and AD3) used in this study were obtained from adult skin punch biopsy (after IRB approval and informed consent) and were cultured in methods previously published[49,57,58]. One adult disease fibroblast line (GM00954, renamed AD1) was obtained from Coriell Institute for Medical Research (Camden, NJ). All procedures were approved by the

Institutional Review Board (IRB #13-001469-AM-00002) and the Embryonic Stem Cell Research Oversight (ESCRO) (ESCRO #2010-010-04A) Committee of the University of California, Los Angeles and informed consent was documented from both patients.

In-vitro derivation and culture of human stem cell lines

The control hiPSC line xc-HUF1 and the three disease hiPSC lines (AD1, AD2, AD3) were developed by reprogramming from corresponding parental fibroblast lines via a lentiviral transduction of a stem cell cassette (STEMCCA) containing the reprogramming factors Oct4, Sox2, Klf4, and c-Myc[59].

Hepatocyte differentiation of induced pluripotent stem cells

To begin hepatocyte differentiation, hiPSCs were passaged at 90% confluency. The next day, the differentiation protocol began as previously published[55].

Immunocytochemistry

Cells were washed with PBS and fixed with 4% paraformaldehyde (Polysciences, Warrington, PA) in 1x PBS for 15 minutes prior to staining. When necessary, samples were permeabilized in 1% Triton X-100 (Sigma-Aldrich, St. Louis, MO) in PBS for 1 hour at room temperature. Subsequently, all samples were blocked with 5% goat serum (Sigma) in PBS for one hour at room temperature. Primary antibodies were diluted to working concentrations in 5% goat serum; cells were incubated with the primary antibody overnight in 4°C. After incubation, cells were washed three times with PBS at 5 minutes per wash. Secondary antibodies were diluted in 5% goat serum and cells were

incubated for 1 hour at RT. Cells were washed three times with PBS and incubated with 1X DAPI (Thermo, Waltham, MA) for 7 minutes. Fluorescence images were captured with an Axiocam MR Monocolor Camera and AxioVision Digital Image Processing Software (Axio Observer Inverted Microscope; Carl Zeiss, Jena, Germany). The primary and secondary antibodies used for hiPSC and hepatocyte-like cells are listed in Table 1.

Teratoma formation and analysis

Teratomas for the control and disease hiPSC lines were generated by injecting 1 x 10^6 cells (resuspended in Matrigel [BD Biosciences]) subcutaneously into both hind limbs of male severe combined immunodeficient (SCID) mice (Charles River Laboratories, San Diego, CA). Tumors were harvested roughly 1-1.5 months after injection and fixed in 4% paraformaldehyde. Tissues were routinely processed and paraffin-embedded followed by staining with hematoxylin and eosin (H&E). All animal experiments adhered to policies set by the UCLA Animal Research Committee and the UCLA Division of Laboratory Animal Medicine (Protocol #2006-119-22).

Karyotype analysis

hiPSCs were cultured to 95-99% confluency in 25 cm^2 flasks and delivered to Cell Line Genetics, Inc. (Madison, WI) for G-band karyotyping analysis.

Reverse transcription-polymerase chain reaction

RNA was extracted from primary fibroblasts, hiPSCs, and hepatocyte-like cells with a Roche High Pure RNA Isolation Kit (Roche Applied Sciences, Indianapolis, IN)

and 10 ng–1 mg was reversed transcribed to cDNA with the Transcriptor First Strand cDNA synthesis kit (Roche Applied Sciences) following the manufacturer's instructions. Primers were designed in NCBI/Primer-Blast and synthesized by Valugene, Inc. (San Diego, CA) and are listed in Table 2. RT-PCR was performed with 25 ng of cDNA from each sample and each reaction was prepared with 12.5 mL 2x KAPA Fast Genotyping Mix (Kapa Biosystems, Wilmington, MA) and with 10 mM forward and reverse primers and was run on a LightCycler 480 Real-Time PCR System (Roche Applied Sciences). Gels were made with 2% agarose (Bio-Rad Laboratories, Hercules, CA) and 1x SYBR Safe DNA Gel Stain (Life Technologies) in tris-acetate-EDTA (TAE) buffer and run on a PowerPac Basic Power Supply (Bio-Rad, Hercules, CA) at 90v for 30 minutes.

Quantitative reverse transcription polymerase chain reaction

Total RNA was isolated from cultures with a Roche High Pure RNA Isolation Kit (Roche Applied Sciences) and 250 ng-1 mg was reverse transcribed to cDNA utilizing a Transcriptor First Strand cDNA Synthesis Kit (Roche Applied Sciences). Primers for endogenous arginase and human codon-optimized arginase and probes (designed from the Roche Universal Probe Library) were synthetized at Valuegene Inc. (Table 3). Quantitative PCR relative gene expression experiments were performed with 10 ng of cDNA on a LightCycler 480 Real-Time PCR System (Roche) and data was analyzed with LightCycler 480 Software (release 1.5.0.). Triplicate experimental samples were paired using the all-to-mean pairing rule ΔCt value calculation with GAPDH for advanced relative quantification.

Cloning and gene optimization

pUC18-HPRTx1-LHA-hEF1α-ArgO-IRES-PAC-HPRTx1-RHA was cloned by PCR of HPRTx1 (Exon 1)-RHA(Right Homologous Arm) with primers 5-HPRT-RHA-NotI (GCATGCGGCCGCCAGTCAGCCCGCGCGCC) and 3-HPRT-RHA-PstI (CGATCTGCAGCCTGCCGCCCTCGCGT) and restriction enzyme digested with NotI and PstI. HPRTx1-LHA (Left-Homologous-Arm) was synthesized by GeneWiz, removed and isolated from pUC57-Kan by digestion with EcoRI and XbaI. hEF1α-ArgO-IRES-PAC was removed and isolated from pRRL-hEF1α-ArgO-IRES-PAC with XbaI+NotI digest. Two synthetic polyadenylation sequences were inserted 3' of HPRTx1-LHA and 5' of HPRTx1-RHA by cutting and inserting the sequences with SpeI and NotI, respectively. Oligonucleotides were synthesized by ValueGene and annealed together to create inserts for cloning. Finally, all inserts were ligated together with pUC18 digested by EcoRI and PstI. DNA was introduced into cells by nucleofection (see Supplemental Experimental Procedures for details).

Human codon optimized arginase (*ArgO*) was developed by running the amino acid sequence of arginase 1 through Gene Designer 2.0 software (DNA2.0, Menlo Park, CA) against the *homo sapiens* codon usage table. Once the initial sequence was produced, it was run through NetGene2 (http://www.cbs.dtu.dk/services/NetGene2/) to find any cryptic splice sites. This sequence was then checked for any long repeats in Oligonucleotides Repeat Finder (http://wwwmgs.bionet.nsc.ru/mgs/programs/oligorep/InpForm.htm). Any variations needed to delete splice sites or long repeats were silent mutations that used the next most common codon in the *Homo sapiens* codon usage table.

Junction PCR and sequencing analysis

To verify targeted integration of our donor vector in corrected hiPSCs, each 5' and 3' junction of the integrated vector was analyzed by PCR and DNA sequencing. Reactions were prepared with genomic DNA, 12.5 mL of Phusion High-Fidelity PCR Master Mix (New England BioLabs, Ipwich, MA), 10.25 mL of water, and 1.25 mL of forward and reverse primers for the 3' and 5' ends of Exon 1 of HPRT (Table 4).

For sequencing, PCR bands were extracted and purified using the Wizard SV Gel and PCR Cleanup System (Promega, Madison WI) and the purified products were sent to Laragen (Culver City, CA) for sequencing analysis.

Functional assay for arginase activity

Arginase activity was measured in cell lysates. 2 x 10^6–4 x 10^6 cells were pelleted by low-speed centrifugation and frozen for each sample. Cell pellets were lysed at 20,000 cells/mL in lysis buffer. Primary tissue sample controls were homogenized with 40 mL of lysis buffer/mg of tissue. Lysis buffer was prepared with 0.1% Triton X-100 and 1x HALT protease inhibitor cocktail (Thermo) and urea production was measured as previously performed[72,73].

Sequencing Analysis

Fibroblasts were cultured in 25 cm^2 flasks and delivered to GeneDx (Gaithersberg, MD) for complete *Arg1* gene sequencing and mutation analysis. Mutations were analyzed in hiPSC and hepatocyte progeny in the UCLA Orphan Disease lab by PCR followed by Sanger sequencing.

Statistical Analysis

All collected data was analyzed with the SPSS (Armonk, NY) statistical package (Version 21.0). Results were expressed as mean ± standard deviation (SD) and p-values were determined using a one-way ANOVA to examine significance across comparisons. Error bars represent SD.

Results

Derivation of patient-specific hiPSCs from arginase-deficient dermal fibroblasts

We derived genetically-distinct hiPSC lines from dermal fibroblasts taken from three patients with hyperargininemia. The first disease dermal fibroblast line, AD1, originating from a female argininemic patient, was purchased from Coriell (GM00954). Two additional dermal fibroblast lines, AD2 and AD3, were derived from skin punch biopsies obtained from a male and female patient, respectively, at UCLA. The AD dermal fibroblasts were successfully reprogrammed to hiPSCs using a lentiviral vector expressing a constitutive polycistronic cassette (STEMCCA) encoding the four transcription factors: *OCT4*, *SOX2*, *KLF4*, and *cMyc*[49,58,60]. Dermal fibroblasts were transduced with the STEMCCA lentivirus and were maintained in culture for 30 days on MEFs before conversion to feeder-free culture conditions. The control hiPSC line (xc-HUF1), derived from the dermal fibroblasts of a healthy adult male, was previously established in the lab using the same reprogramming methodology[57].

AD1, AD2, and AD3 hiPSC lines exhibited normal stem cell-like morphology throughout the course of the study. Characterization of the AD hiPSCs included immunophenotyping for common pluripotent stem cell markers, alkaline phosphatase

staining, *in vivo* teratoma formation, and karyotype analysis. AD1, AD2, and AD3 hiPSCs stained positive for pluripotency markers: *Oct4, NANOG, SSEA-3, SSEA-4, Tra-1-60, Tra-1-81* and all exhibited positive alkaline phosphatase activity (Figure 2-1). Normal karyotypic analyses, with no genomic abnormalities, were detected through G-banding studies of AD1, AD2, and AD3 hiPSC lines (Figure 2-2). Furthermore, AD hiPSCs were collected and injected subcutaneously into the hindleg of SCID mice for *in vivo* teratoma analysis. Teratoma sections from AD1, AD2, and AD3 were stained with H&E and exhibited formation of gut (endoderm), neuroectoderm (ectoderm), and chondrocyte (mesoderm) derivatives, demonstrating the ability of our hiPSCs to form tissues from all three germ layers (Figure 2-2). Additionally, the specific arginase mutations were determined for each line (Figure 2-3). Characterization of all three disease hiPSCs were compared to non-disease controls H9 hESCs (data not shown) and xc-HUF1 hiPSCs and demonstrated no difference in pluripotency profile.

Design of ArgO and vectors for gene correction of hiPSCs

To correct for the mutant *Arg1* gene in our patient-derived AD hiPSCs, we designed a selectable, full-length codon-optimized human arginase cDNA (*ArgO*) expression cassette under the constitutive control of the human elongation factor 1a (hEF1a) promoter, referred to as LEAPR (**L**eft homologous arm-h**E**F1a-**A**rgO-IRES-**P**uro(R)-**R**ight homologous arm), to be inserted into Exon 1 of the HPRT locus (Figure 2-4). Utilizing CRISPR/Cas9 nickases to bind and cleave Exon 1 of HPRT, we achieved targeted LEAPR addition into the desired site. LEAPR addition and disruption of the HPRT locus allowed for secondary positive clonal selection of successful on-target

integration via resistance to 6-thioguanine (6-TG) treatment. Additionally, a puromycin resistance gene encoded within the LEAPR construct afforded the ability to utilize an efficient dual selection method to isolate a clonal population of cells that successfully integrated our vector into the HPRT locus. After dual selection with puromycin and 6-TG, AD1, AD2, and AD3 hiPSCs maintained normal stem cell-like morphology (Figure 2-5).

Evaluation of Targeted Integration and Expression of ArgO into Corrected hiPSCs

After delivery of the LEAPR construct (Figure 2-4), we performed experiments to verify correct on-target integration into the AD hiPSCs. AD hiPSCs were first dual-selected by two cycles of 1 μg/mL puromycin treatment for 72 hours followed by 6-TG treatment. Dual-resistant cell populations were then clonally selected into three subclones each for all AD hiPSC lines. To analyze the targeted integration of our donor vector into Exon 1 of the HPRT locus, primers were designed to span each junction between the endogenous genome and our inserted vector. For each junction, one primer was designed to bind a region of the genome outside of the homologous arm region, and another was designed to bind a sequence within our inserted donor vector. Products at both 5' and 3' junction sites demonstrated on-target integration of our LEAPR construct in each of three subclones of the corrected AD1, AD2, and AD3 hiPSC lines (Figure 2-6). Additionally, sequencing analysis of the junction PCR products showed the seamless transition between donor vector sequence and the endogenous genome sequence of our gene-corrected cell lines at both the 5' and 3' junctions of our gene cassette insert (Figure 2-7).

Arginase levels were examined in the LEAPR-corrected hiPSC lines by measuring RNA expression via qRT-PCR and functionality via urea production. After puromycin and 6-TG selection, corrected hiPSCs (n = 3) expressed significantly higher RNA levels ($p < 0.0001$) of codon optimized arginase compared to wild type arginase RNA levels in uncorrected AD hiPSCs, demonstrating expression in all three corrected hiPSC lines. The integration of *ArgO* increased arginase levels in AD1, AD2, and AD3 hiPSCs to 58%, 92%, and 46% respectively when compared to wild type arginase levels in human fetal liver (Figure 2-8). Additionally, corrected AD hiPSCs (n = 2) exhibited a significant increase ($p < 0.0001$) in urea production when compared to their uncorrected counterparts. Functionality of corrected AD1 hiPSCs (n = 2) increased to 102% ($p = 0.0212$) of that measured in human fetal liver levels (Figure 2-8). Varying degrees of recovery were observed in AD1, AD2, and AD3 corrected lines; however, the lowest recorded recovery level was still 71% of the primary fetal liver (Figure 2-8). Taken together, these data demonstrate a high specificity of integration into Exon 1 of the *HPRT* target site as well as a high codon optimized arginase RNA expression and a restoration of substantial functional arginase activity in hiPSCs.

Directed differentiation of human pluripotent cells into hepatocyte-like cells

Using a previously published protocol[55], we differentiated the corrected AD1, AD2, and AD3 hiPSCs, their uncorrected counterparts, H9 hESCs (data not shown) and control xc-HUF1 hiPSCs into hepatocyte-like cells. After 21 days, we assessed expression of specific liver markers and assessed liver cell-specific functions of our derivatives. Morphology of the genetically modified AD1 hepatocyte-like cells resembled

both that of their uncorrected counterparts (AD1 WT hepatocytes), and primary human adult hepatocytes (Figures 2-9, 2-10).

At the end of the final differentiation stage, we characterized the expression of hepatic markers in our derivatives. Similar to the primary adult hepatocyte control, LEAPR-corrected AD1, AD2, and AD3 derivatives stained positive for albumin (Figures 2-9, 2-10). The hepatocyte-like cells exhibited expression of *AFP*, whereas the primary adult hepatocyte control was essentially negative for *AFP*. This observation is consistent with previous studies demonstrating that PSC-derived hepatocyte-like cells more closely mimic fetal as opposed to adult hepatocytes; mature hepatocytes lose *AFP* expression while more fetal-like hepatocytes continue to express *AFP*. Therefore, we compared RNA expression of multiple hepatic-specific markers of the derivatives to a human fetal liver control. RT-PCR analysis showed that AD1, AD2, and AD3 hepatocyte-like cells all expressed hepatic functional genes including: *ALB, AFP, AAT, CK18, CPS1, CYP3A4, FIX, TF, TDO2,* and *UDP-GT* (Figures 2-11, 2-12). Human primary adult hepatocytes and fetal liver were used as positive controls for the immunostaining and RT-PCR analysis, respectively.

Additionally, we assessed liver-specific functionality of both our genetically modified and unmodified AD1, AD2, and AD3 hepatocyte-like cells. At day 21, we measured glycogen storage via Periodic Acid-Schiff (PAS) staining of all hepatic derivatives. Similar to primary adult hepatocytes, corrected AD1, AD2, and AD3 hepatocyte-like cells stained positive by PAS (Figures 2-9, 2-10). These results demonstrate that genetic modification of hiPSCs with our LEAPR construct does not interfere with the capability of the cells to differentiate into hepatocyte-like cells.

Evaluation of arginase expression and functionality in hepatocyte-like cells

We examined codon optimized arginase RNA expression and functionality in the hiPSC-derived hepatocyte-like cells to determine the maintenance of arginase expression after directed differentiation. After the final differentiation step, RNA was collected from LEAPR-corrected AD1, AD2, and AD3 hepatocyte-like cells and arginase mRNA levels were quantified and compared to both corrected hiPSC and fetal liver levels via qRT-PCR. Hepatic differentiation did result in a significant decrease ($p < 0.0001$ for AD1 and AD2; $p < 0.0002$ for AD3) in arginase mRNA expression in all three LEAPR-corrected hepatocyte-like cell lines compared to undifferentiated hiPSCs (Figure 2-13). However, despite the decline in expression compared to hiPSCs, AD1, AD2, and AD3 hepatocyte-like cells maintained arginase mRNA levels of 27%, 39%, and 36% of fetal liver *Arg1* levels.

With the above findings, an expected post-differentiation decline was also observed in arginase functionality ($p = 0.0004$ for AD1; $p = 0.001$ for AD2; $p = 0.0007$ for AD3 compared to corrected hiPSCs) of the LEAPR derivatives. Urea production in AD1, AD2, and AD3 LEAPR-corrected hepatocyte-like cells declined 61%, 37%, and 38% of levels measured in hiPSCs; however, all three corrected hepatocyte-like cell lines maintained > 40% of urea production of fetal liver (Figure 2-13).

Discussion

Chronic therapy for urea cycle disorders includes dietary restriction to limit nitrogen intake and pharmacological intervention with nitrogen scavenging drugs (e.g. phenylbutyrate). Such substrate restriction is commonly used for treating urea cycle

disorders and while it is somewhat effective, this therapy is more prophylactic than curative and patients remain at risk for developing long-term neurological issues due to intermittent hyperammonemia. Gene and stem cell therapy have emerged as promising alterative therapeutic avenues to treat these disorders and prevent the development of hyperammonemia-induced neurological injury[61,62,63,64,65].

Stem cells, specifically hiPSCs, provide in principle, a functionally inexhaustible source of patient-specific cells that can undergo directed differentiation into various somatic cell types to be used for cellular replacement therapies[66,67,68]. Due to their therapeutic potential, considerable effort has been expended to optimize protocols to genetically modify these cells in order to model disease and to use in potential cellular therapies[69]. However, despite the promise of utilizing genetically modified hiPSCs for therapeutic studies, the ability to efficiently deliver genes to targeted sites in hiPSCs is hampered by several challenges. Non-viral methods, such as chemical transfection or electroporation, and viral methods, via lentiviruses or adeno-associated virus (AAVs), all suffer from relatively low transfection and transduction efficiencies, transient expression, and off-target integration in the host hiPSC genome[65,69]. Recently, the development of highly specific clustered interspaced short palindromic repeats (CRISPRs) and CRISPR-associated (Cas) systems to introduce genes into hiPSCs have begun to address many previous issues surrounding genomic editing of stem cells. Unlike its predecessors zinc finger nucleases (ZFNs) and transcription activator-like effector nucleases (TALENs), CRISPR/Cas9 can be produced rapidly and introduced into specific target sites with increased accuracy[6,70,71]. As such, recent studies have demonstrated highly

efficient genetic correction of hiPSCs utilizing CRISPR/Cas9 for neural and muscular disorders[8].

The goal of the present study was to determine if integration of codon-optimized arginase into genetically distinct patient-specific hiPSCs could produce *in vitro* enzyme function after differentiation into hepatocyte-like derivatives for potential use in cellular therapy for these patients. Previous gene therapy studies have demonstrated successful reversal of disease manifestations through either treatment of neonatal mice with a helper-dependent adenoviral vector (HDV) or with AAV-expressing arginase [63,72]. In the former, the transient nature of expression led to loss of arginase function and in the later, long-term survival without neuropathology was achieved; however, with the loss of episomal genomes, the level of arginase expression was low and, therefore, the animals remained nitrogen vulnerable[73]. However, these murine studies were able to determine both that long-term survival with normal behavior and learning was possible and that only low levels of hepatic arginase activity, as low as 3.5-5%, were necessary to prevent brain injury and/or death from hyperammonemia or hyperargininemia[72,73,74]. Here, we developed a CRISPR/Cas9-based strategy to deliver a codon-optimized version of human arginase 1 into hiPSCs derived from arginase deficient patients. Arginase 1 was introduced into Exon 1 of the HPRT locus via a construct containing right and left homologous arms, the human elongation factor 1a promoter, a polyadenylation signal, and puromycin for selection (LEAPR). Successful integration resulted in substantial arginase activity in hiPSCs and in their differentiated derivatives.

Cellular HPRT is an enzyme that catalyzes the conversion of hypoxanthine to inosine monophosphate and guanine to guanosine monophosphate in the non-essential

purine salvage pathway[75]. Homozygous loss of HPRT function results in Lesch-Nyhan syndrome, which causes an overproduction of uric acid. However, in normal conditions, purine salvage and HPRT do not play a major role in cell growth and proliferation; in therapeutic administration of cells where HPRT is not functional in the large mass of HPRT-positive cells (such as the liver), it is believed that this loss will be inconsequential in purine metabolism[76]. There are certainly desirable selective advantages for utilization of the HPRT locus for integrated cell selection: HPRT-positive cells are sensitive to 6-thioguanine (6-TG); this property allows for selection with 6-TG after HPRT locus disruption[77,78,79]. Transfection efficiency of hiPSCs is inherently low; the incorporation of a dual selection method with puromycin and 6-TG allowed us to purify a population of hiPSCs that contained the integrated construct at the targeted site utilizing nucleofection to deliver CRISPR/Cas9 nickases and the LEAPR cassette. In culture, these corrected hiPSCs maintained proper morphology and pluripotency, and sequencing confirmed that the constructs integrated into the correct target site in HPRT.

Importantly, arginase was highly expressed in LEAPR-corrected cells as shown by both qRT-PCR and in urea production from functional arginase activity. After directed differentiation of LEAPR-corrected hiPSCs to the hepatic lineage, the hepatocyte-like cells were positive for albumin and a-fetoprotein, stored glycogen, and expressed multiple liver-specific RNAs. To determine if differentiation affected expression and functionality of arginase in the hepatocyte-like cells, we quantified RNA levels and urea production for comparison with their hiPSC counterparts. While RNA levels of LEAPR-

derived arginase in hepatocyte-like cells were lower when compared to their hiPSC counterparts, functional arginase expression with urea production for all LEAPR-corrected hepatocyte-like cells remained. Previous studies have shown a decline occurs in transgene expression during differentiation with the use of the hEF1a promoter in embryonic stem cells, and this in part may explain in part the decline in expression in the hepatocyte derivatives in this study[80]. In aggregate, however, these data demonstrate that genetic modification at the HPRT locus of the arginase-deficient lines had no deleterious effect on their pluripotent capability and overall "stemness"; were not altered by nucleofection, selection, or culture of the hiPSCs; and were able to be differentiated into hepatocytes with restoration of arginase activity.

Based on these data, integration of arginase 1 via the LEAPR expression construct by targeting the HPRT locus demonstrates the potential for restoring enzymatic activity in cells derived from hyperargininemic patients. Previously, we have shown in a murine model that with relatively low overall hepatic arginase activity that urea cycle function at 3.5-5% of normal led to long-term survival with controlled plasma arginine and ammonia; however these animals remained nitrogen vulnerable due to the low level of arginase expression[73]. LEAPR-corrected hepatocyte-like cells across all three lines demonstrated functionality of at least 40% compared to fetal liver; while the EF1a promoter-based expression has been demonstrated previously to result in robust expression at each stage of ES cell differentiation (at least in mice), transgene expression is known to decline with cellular differentiation[80]. However, arginase expression remains well above the minimum threshold needed for survival and adequate nitrogen metabolism determined from the prior murine arginase studies[73].

Over the last 30 years, multiple studies in rodents have shown that adult hepatocyte transplantation can reverse liver failure and can correct various metabolic deficiencies of the liver[81,82]. While clinical trials of hepatocyte transplantation have demonstrated the long-term safety of cellular administration, only partial correction of metabolic disorders in humans has been achieved[83,84]. In part due to the limited availability of fresh donor hepatocytes of adequate quality, clinical trials have been hampered and reports have been limited in general to case reports involving at most a few patients and generally with no untreated controls[85,86,87,88]. While attaining adequate engraftment will need further attention to make such therapies successful for patients with metabolic liver disorders, issues of cellular rejection should be greatly reduced with an hiPSC approach as described herein[81].

In choosing this approach where cell availability and numbers of hepatocytes will not be a limitation, there are other important implications for treating more common monogenic disorders of the liver. The safe harbor of Exon 1 of HPRT could be used in that the efficiency of homologous recombination has been demonstrated here as well as the exogenous gene expression at this locus based on the hEF1a promoter. Targeted therapy of other liver-based disorders would be easily addressed by substitution of the arginase cDNA from the donor construct with one of the other enzyme sequences in another metabolic disorder.

This study presents an approach that can be utilized to integrate an optimized cassette into a universal site distant from proto-oncogenes in patient-specific hiPSCs to restore function of abnormal liver enzymes. While we have addressed the restoration and maintenance of transgene expression pre- and post-differentiation, additional

studies are required to investigate the *in vivo* therapeutic efficacy of the corrected derivatives to maintain recovered arginase activity after cellular transplantation. Successful *in vivo* recovery of enzyme function by means of these strategies could benefit enzyme deficiencies of the urea cycle and other inborn errors of metabolism.

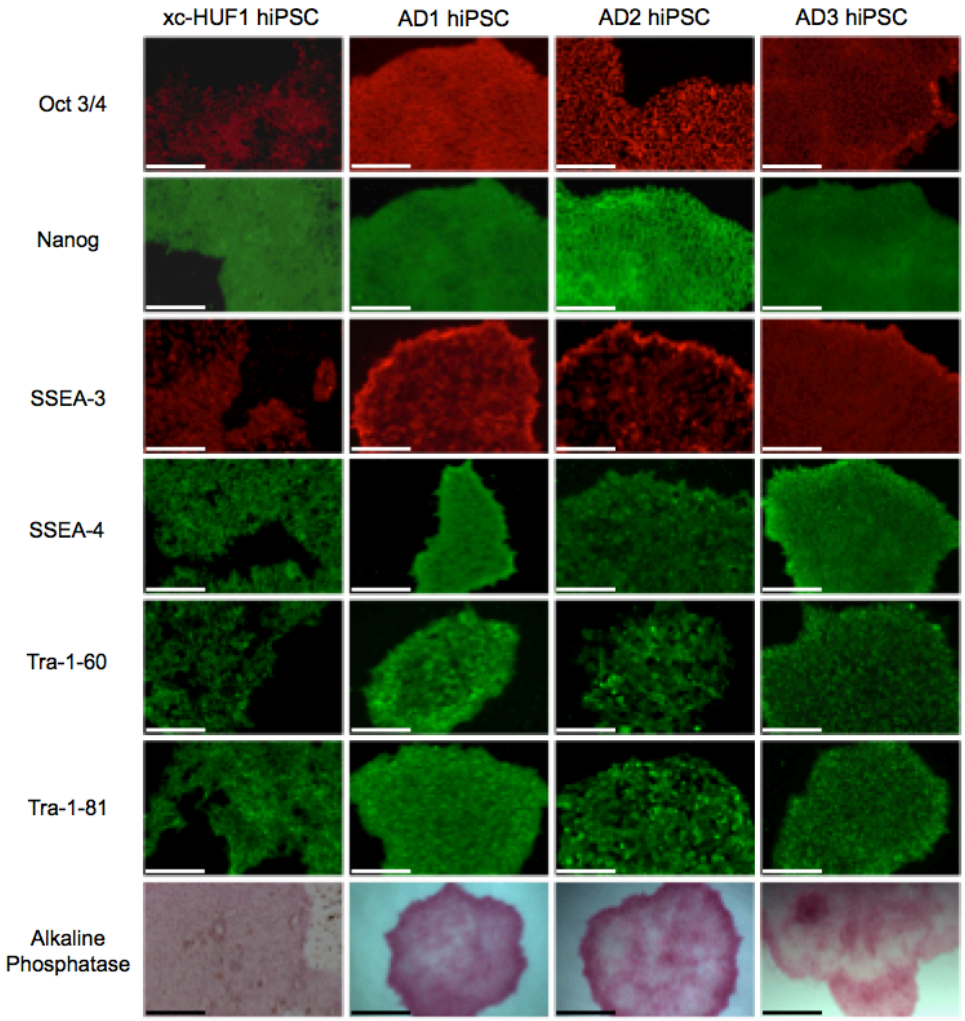

Figure 2-1. Pluripotency characterization of arginase deficient (AD) hiPSCs

Pluripotency of all three AD hiPSC lines was measured via immunophenotyping. AD1, AD2, and AD3 subclones were positive for octamer-binding transcription factor-4 (OCT3/4), homeobox protein nanog (NANOG), stage-specific embryonic antigens 3 (SSEA-3) and 4 (SSEA-4), tumor-related antigens 1-60 (TRA-1-60) and 1-81 (TRA-1-81), and alkaline phosphatase. AD hiPSCs were compared to a wild type hiPSC line xc-HUF1. (Scale bars for all images are 200 mm except alkaline phosphatase which is 500 mm.)

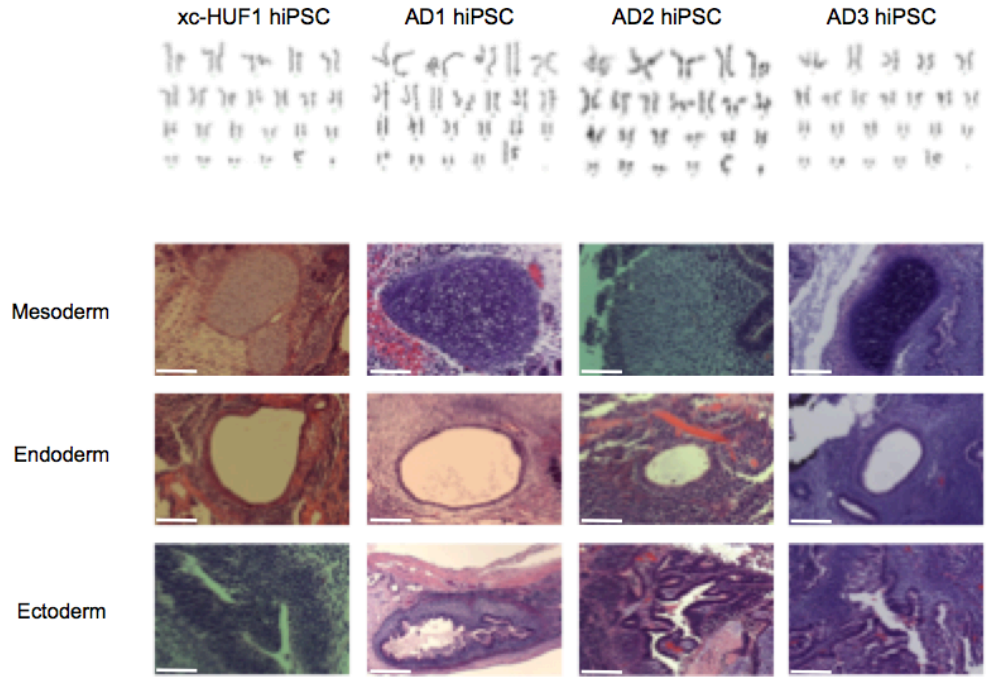

Figure 2-2. Karyotype and teratoma characterization of AD hiPSCs

Pluripotency of all three AD hiPSC lines was measured via immunophenotyping. AD1, AD2, and AD3 subclones were positive for octamer-binding transcription factor-4 (OCT3/4), homeobox protein nanog (NANOG), stage-specific embryonic antigens 3 (SSEA-3) and 4 (SSEA-4), tumor-related antigens 1-60 (TRA-1-60) and 1-81 (TRA-1-81), and alkaline phosphatase. AD hiPSCs were compared to a wild type hiPSC line xc-HUF1. (Scale bars for all images are 200 mm except alkaline phosphatase, which is 500 mm.)

Line	Source	Mutation	Notes
AD1	Coriell GM00954	1. G>C p.Ala298Pro 2. C>T p.Arg21Ter	Female, Hispanic, 4 years old 1. Heterozygous, disease causing
AD2	UCLA	1. c.61 C>T p.Arg21Ter(R21X) 2. c.709 G>A p.Asp237Asn (D237N)	Male, Asian, 23 years old 1. Heterozygous, disease causing 2. Heterozygous, disease causing
AD3	UCLA	1. c.365 G>A p.Trp122Ter (W122X)	Female, Hispanic, 52 years old 1. Homozygous, disease causing

Figure 2-3. Arginase mutations in AD patient samples

Sequencing analysis reveals specific arginase mutations in each AD1, AD2, and AD3 lines.

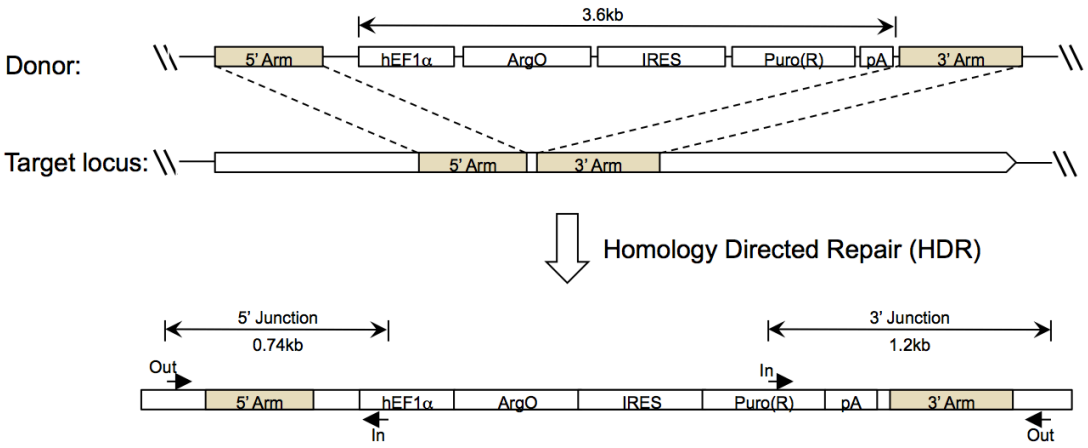

Figure 2-4. Design and integration of LEAPR expression cassette

Design of the LEAPR construct containing the human codon optimized arginase (*ArgO*).

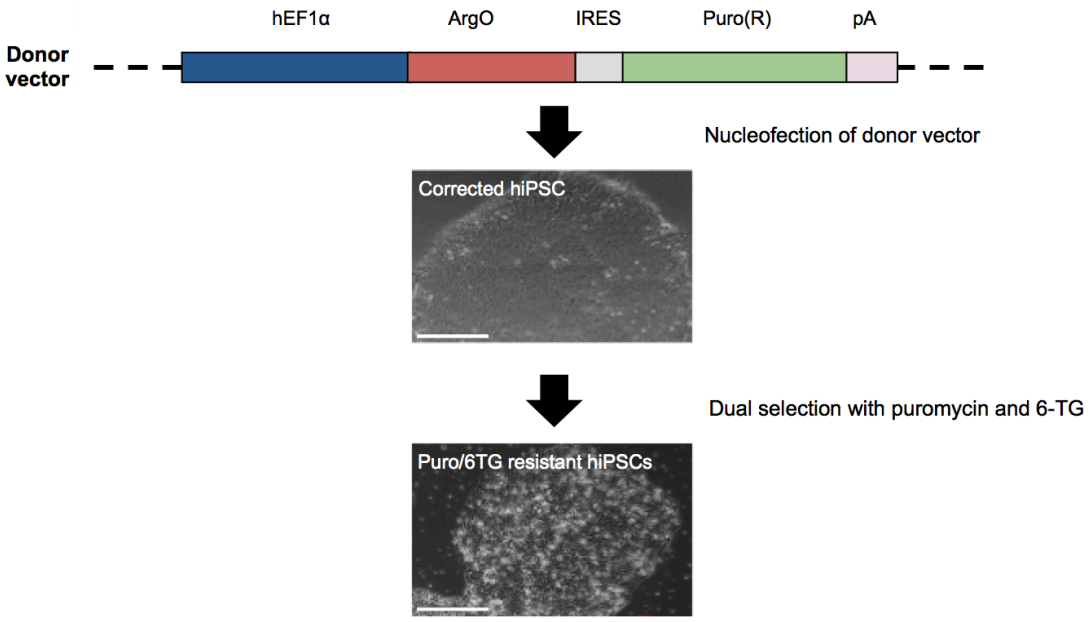

Figure 2-5. Dual selection of corrected hiPSCs with puromycin and 6-TG

Corrected AD hiPSCs selected with puromycin and 6-TG dual treatment maintained normal morphology

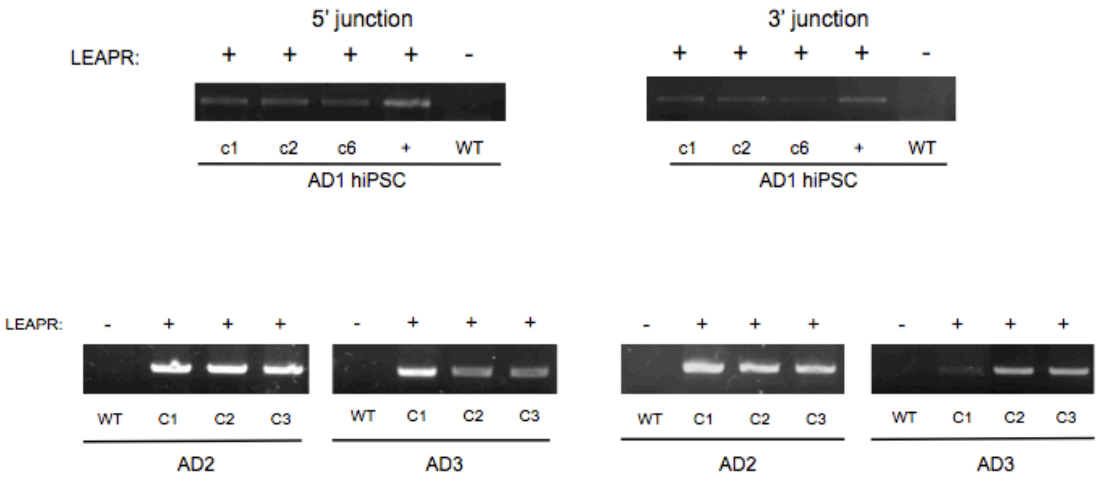

Figure 2-6. Junction PCRs demonstrate targeted integration of *ArgO*

Junction PCR shows integration of the construct in AD1, AD2, and AD3 hiPSCs in Exon 1 of the HPRT site.

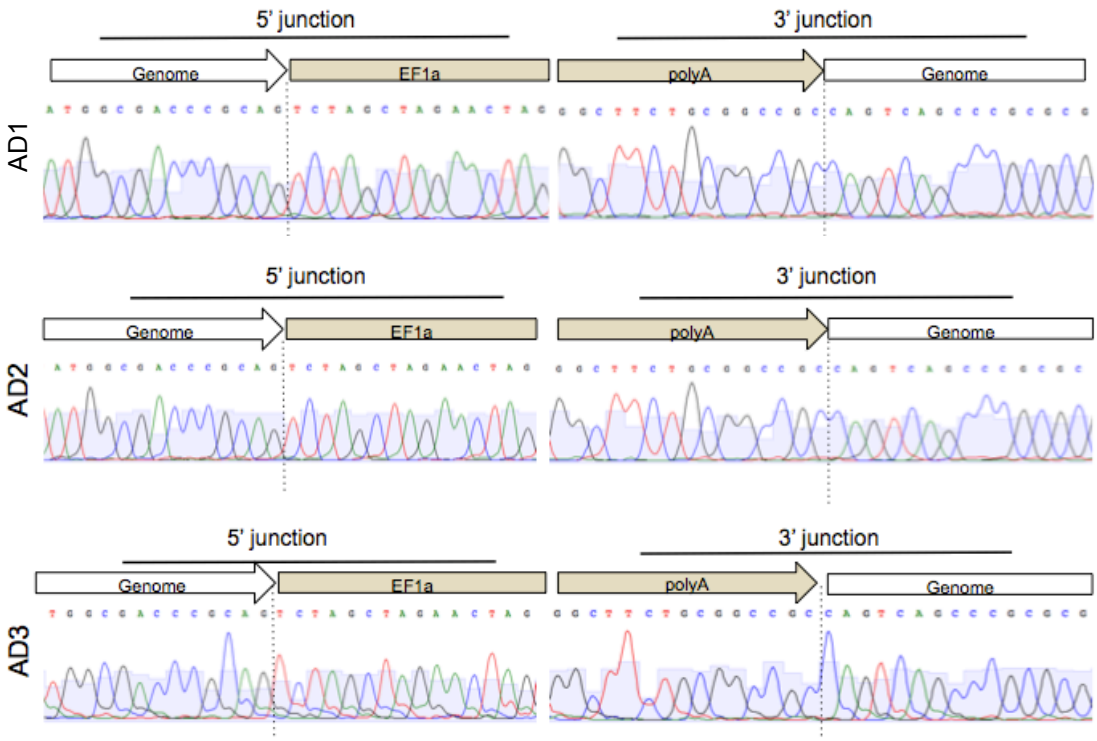

Figure 2-7. Sequencing for *ArgO*

Sequencing analysis demonstrates seamless integration of the construct in AD1, AD2, and AD3 hiPSCs at the target site.

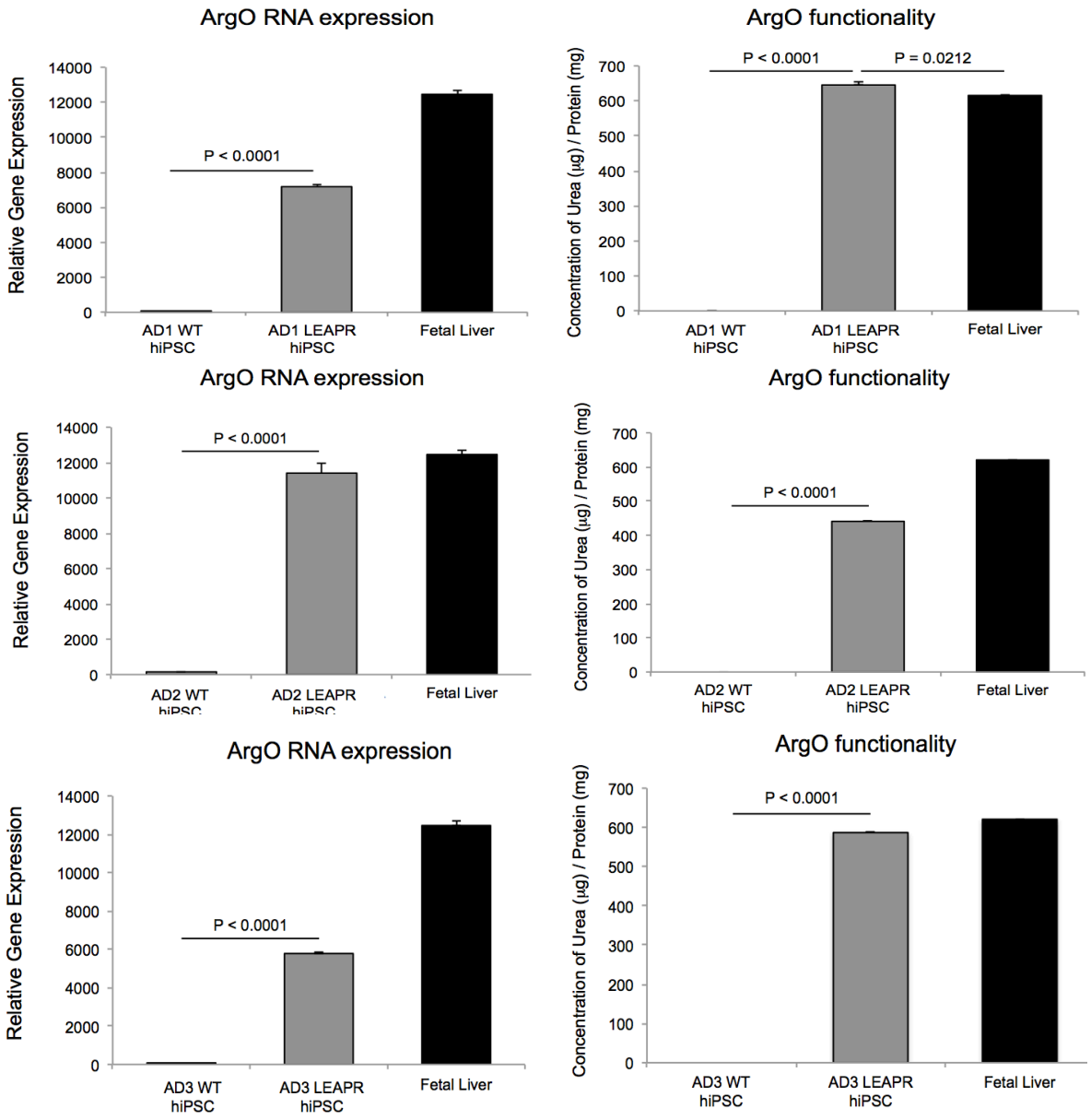

Figure 2-8. Expression and functionality of ArgO in AD hiPSCs

Relative gene expression of *ArgO*, measured against glyceraldehyde 3-phosphate dehydrogenase (GAPDH), in AD1 uncorrected and corrected hiPSCs was measured by qRT-PCR. After integration of LEAPR into Exon 1 of the HPRT site, codon-optimized arginase expression in AD1, AD2, and AD3 was measured at 58%, 92%, 46%, respectively, of wild type *Arg1* levels in fetal liver (right). Additionally, addition of *ArgO* increased argianse function by at least 71% in AD hiPSCs (left).

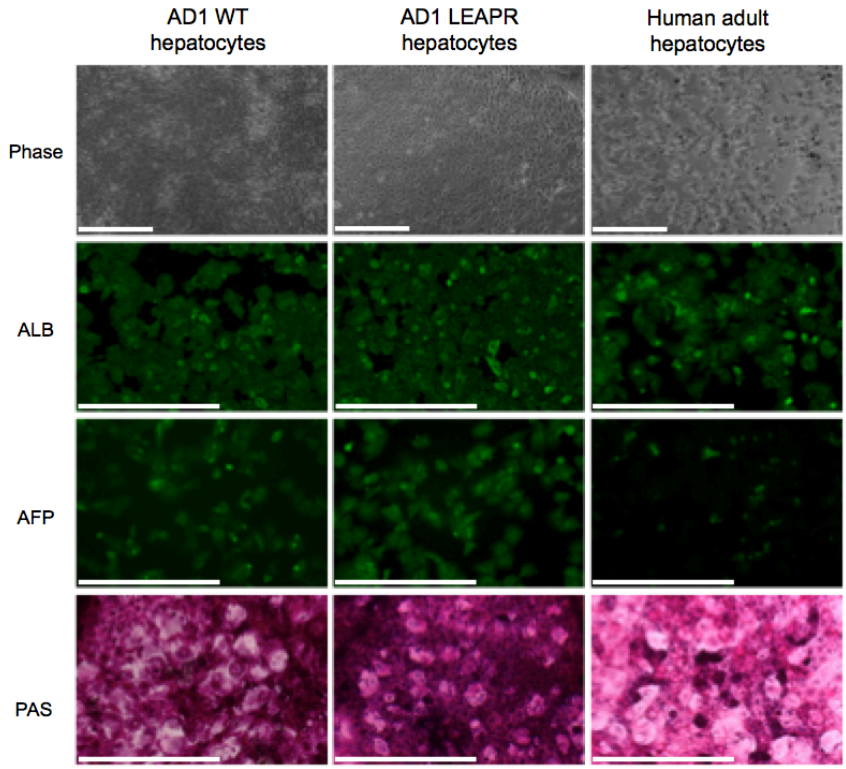

Figure 2-9. Characterization of AD1 hepatocyte-like cells

Derived uncorrected and corrected AD1 hepatocyte-like cells maintained similar morphology compared to primary adult hepatocytes *in-vitro*. Hepatocyte-like cells were positive for both albumin and alpha-fetoprotein (*AFP*), suggesting that they present as more fetal in phenotype. Additionally, derived hepatocyte-like cells exhibit active glycogen storage, as measured by Periodic Acid Schiff (PAS) staining. (Scale bars = 500 mm)

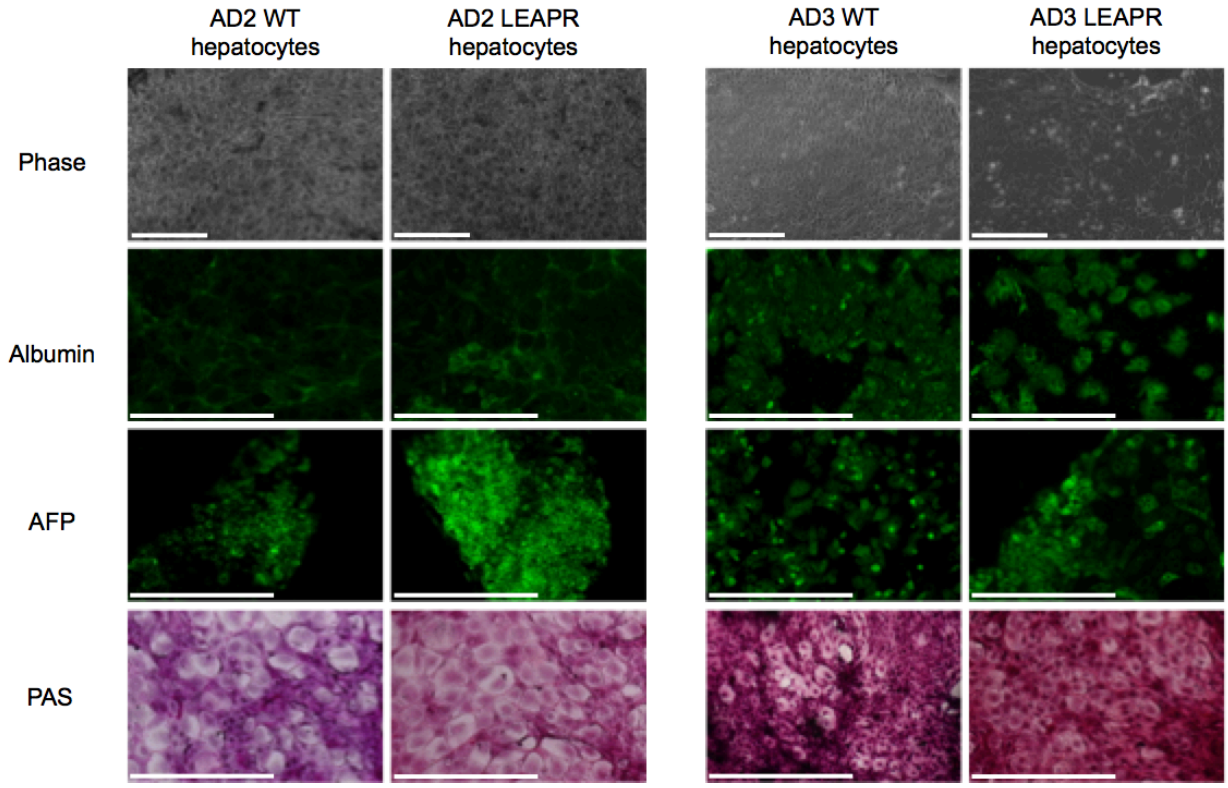

Figure 2-10. Characterization of AD2 and AD3 hepatocyte-like cells

Derived uncorrected and corrected AD2 and AD3 hepatocyte-like cells maintained similar morphology compared to primary adult hepatocytes *in-vitro*. Hepatocyte-like cells were positive for both albumin and alpha-fetoprotein (*AFP*), suggesting that they present as more fetal in phenotype. Additionally, derived hepatocyte-like cells exhibit active glycogen storage, as measured by Periodic Acid Schiff (PAS) staining. (Scale bars = 500 mm)

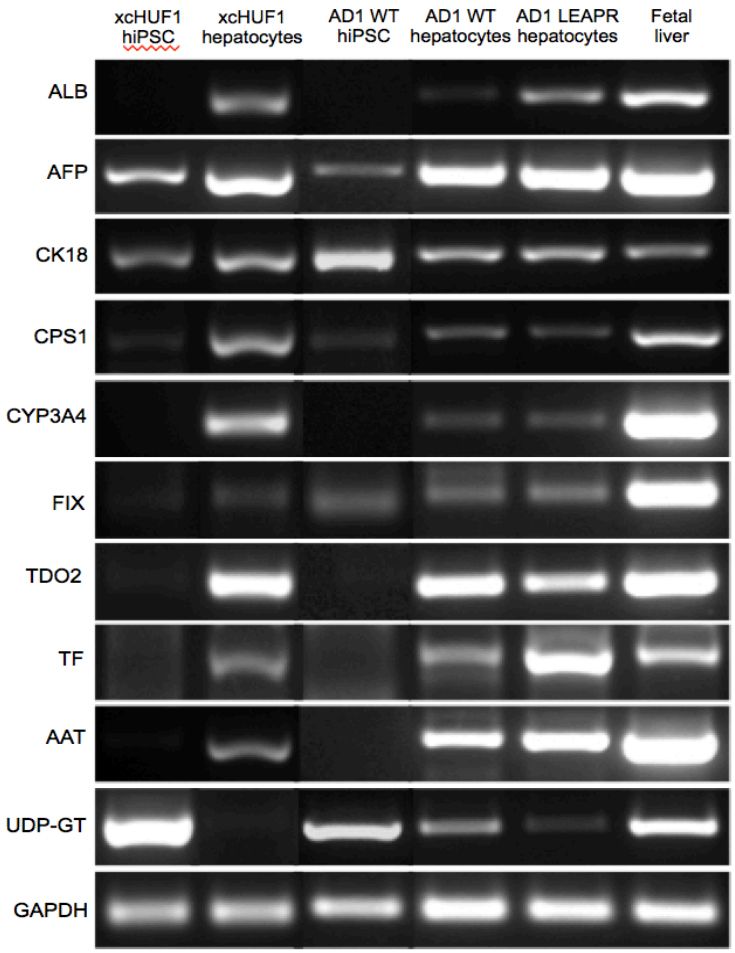

Figure 2-11. Hepatic gene expression of xcHUF1 and AD1 hepatocyte-like cells

Both uncorrected and corrected AD1, as well as wild-type xcHUF1, hepatocyte-like cells express hepatic markers: alpha 1-antitrypsin (*AAT*), *AFP*, human serum albumin (*ALB*), cytokeratin 18 (CK18), carbamoyl phosphate synthase 1 (*CPS1*), cytochrome p450 3A4 (*CYP3A4*), factor IX (*FIX*), transferrin (*TF*), tryptophan 2,3-dioxygenase (*TDO2*), and uridine diphosphate glucuronyltransferase (*UDP-GT*).

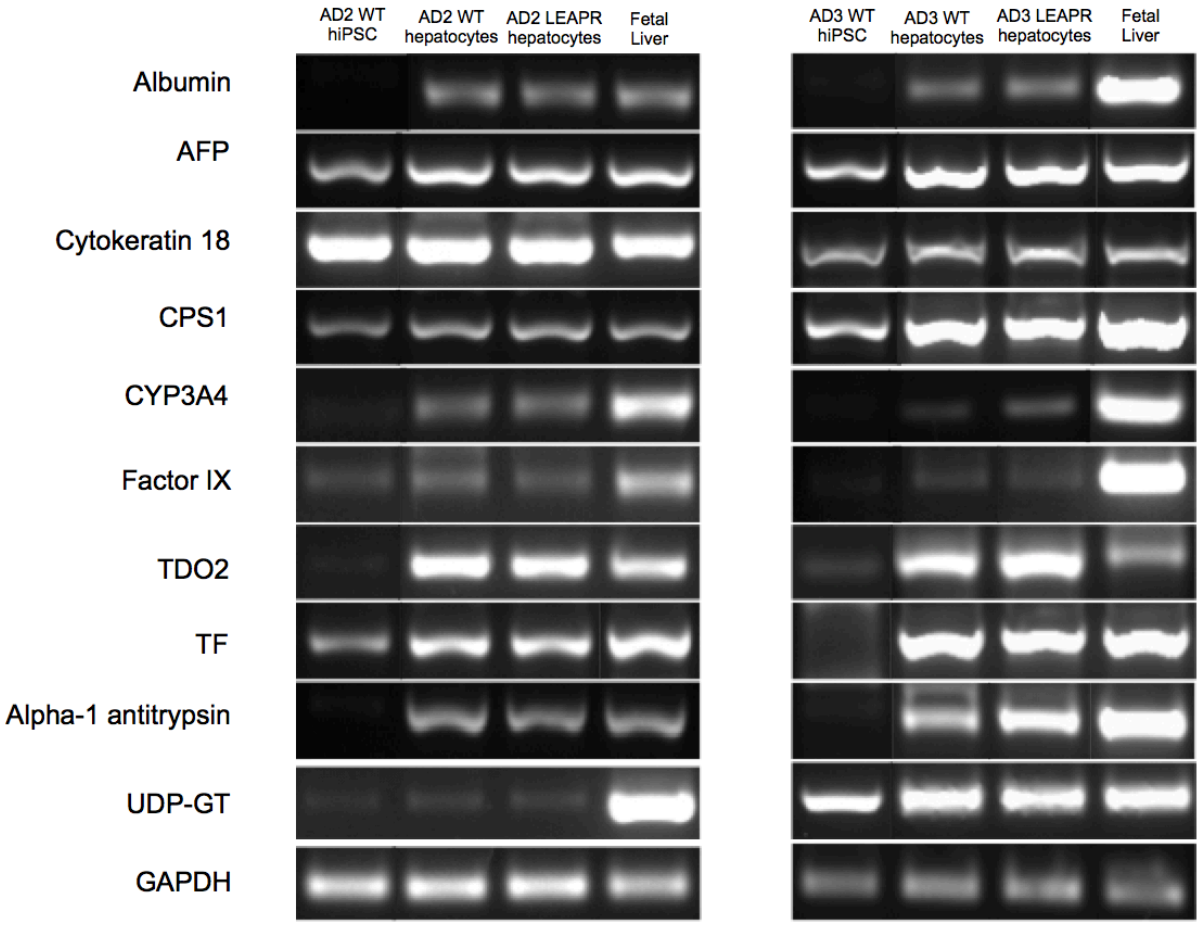

Figure 2-12. Hepatic gene expression of AD2 and AD3 hepatocyte-like cells

Both uncorrected and corrected AD2 and AD3 hepatocyte-like cells express hepatic markers: alpha 1-antitrypsin (*AAT*), *AFP*, human serum albumin (*ALB*), cytokeratin 18 (CK18), carbamoyl phosphate synthase 1 (*CPS1*), cytochrome p450 3A4 (*CYP3A4*), factor IX (*FIX*), transferrin (*TF*), tryptophan 2,3-dioxygenase (*TDO2*), and uridine diphosphate glucuronyltransferase (*UDP-GT*).

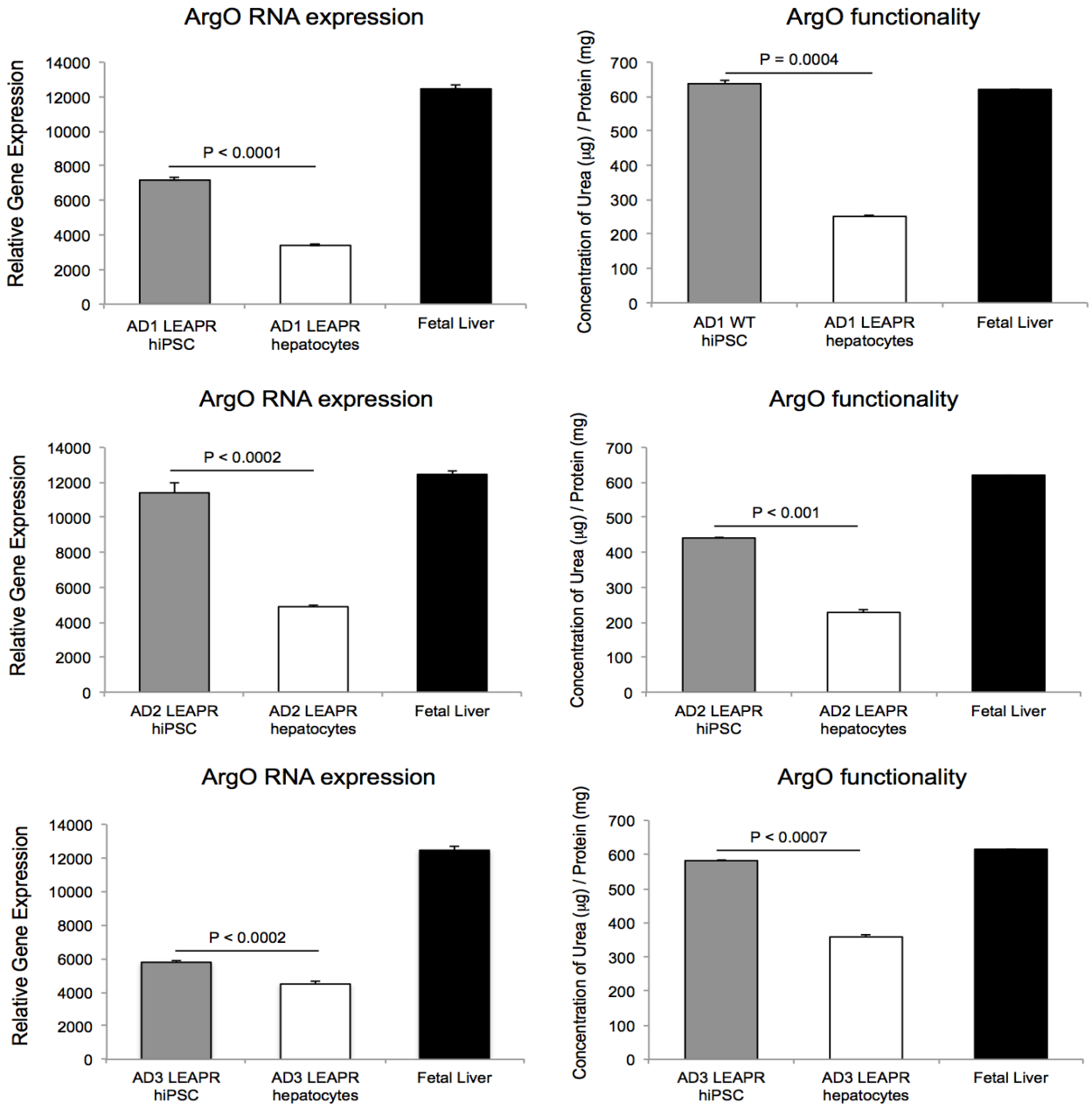

Figure 2-13. Expression and functionality of ArgO in AD hepatocytes

mRNA levels of *ArgO* in AD1, AD2, and AD3 hepatocyte-like cells decrease compared to hiPSCs; however, expression is maintained, compared to fetal liver, at 27%, 39%, and 36% respectively, well above the 5% recovery necessary to maintain survival of mice *in vivo*. Urea production of corrected AD1, AD2, and AD3 hepatocyte-like cells also decreases post-differentiation 61%, 38%, and 37%, but still function at least 40% of fetal liver levels.

Conclusions and Future Directions

Stem cell research holds great promise in advancing both disease research and cellular therapies. Specifically, the ability to reprogram human dermal fibroblasts, and other accessible adult cell types, into induced pluripotent stem cells makes autologous cell therapies and personalized medicine more of a reality than before. However, despite the versatility and potential of stem cell technology, there are still numerous challenges that must be addressed before it can be counted on as a viable therapeutic option. The work presented here addresses two major constraints that limit the therapeutic applicability of stem cells: genomic instability and efficient genetic correction of hiPSCs. We have demonstrated that 1) lower endogenous pools of dNTPs in hiPSCS may promote RS-induced DNA damage and cellular genomic instability, but exogenous supplementation of deoxynucleosides can augment dNTP pools and alleviate incidence of genomic damage and 2) a human codon-optimized arginase gene can be efficiently introduced, via CRISPR/Cas9 technology, into the HPRT gene in hiPSCs and can recover enzyme function in hiPSCs and hepatocyte-like derivatives.

Nucleoside supplementation restores dNTP balance and alleviates genomic instability in hiPSCs

In this study, we demonstrated, in three genetically distinct lines, that hiPSCs have lower endogenous pools of dCTP, dTTP, dATP, and dTTP and higher levels of DNA damage compared to their parental somatic cells. Maintaining a balance of endogenous dNTPs is essential for proper DNA replication and repair; therefore, given that hiPSCs have increased replication kinetics and altered DNA damage checkpoints, lowered dNTP pools may contribute to increased RS and genomic damage. To our

knowledge, this is the first study that has investigated a link between dNTP pools and DNA damage in hiPSCs.

Furthermore, we show that supplementation of culture media with exogenous deoxynucleosides can significantly augment dCTP, dTTP, dGTP, and dATP pools, reduce incidence of DNA damage, and potentially prevent long-term, culture-induced genomic instability in all hiPSC lines. Previous studies have shown that supplementation with ribonucleosides can alleviate DNA damage and reduce incidence of CNVs; however, we have demonstrated that a custom cocktail of dNs can have a greater effect. Preliminary data also suggests that supplementation with dNs results in a greater reduction in DNA damage compared to supplementation with antioxidants; however, additional studies are required to investigate the effects of a combination of antioxidant and nucleoside supplementation to alleviate ROS and RS-induced genomic instability (Supplementary Figure 1-1).

Even though we have demonstrated a possible solution for preventing genomic instability in hiPSCs, further studies are needed to investigate the effect that dN supplementation has on cell cycle kinetics, reprogramming, differentiation of hiPSCs. We have shown that nucleoside supplementation has the potential to increase efficiency of hiPSC reprogramming and differentiation; however, it is still unclear if these results are replicable or artifacts of culture (Supplementary Figures 1-2, 1-3). Also, elucidating the effects of exonenous supplementation on cell cycle kinetics and DNA repair can contribute to the field's understanding of cellular mechanisms of stem cells, which would aid in the derivation of universally applicable, culture-based tools to maintain genomic stability of hiPSCs.

Restoring ureagenesis in hepatocytes by CRISPR/Cas9-mediated genomic addition to arginase-deficient induced pluripotent stem cells

Our second goal was to demonstrate successful and efficient targeted integration of a human codon optimized arginase gene, utilizing CRISPR/Cas9, into arginase deficient hiPSCs to recover enzyme function. We delivered ArgO into Exon 1 of the HPRT gene in three genetically distinct arginase deficient hiPSC lines, and the corrected cells were dual selected with puromycin and 6-TG. Integration into the targeted site was confirmed via junction PCR and sequencing, and the ArgO was able siginificantly to recover arginase activity in the disease lines. Furthermore, hepatocyte-like cells derived from the corrected hiPSCs maintained arginase activity and expression well above the minimum threshold necessary for *in vivo* studies.

However, arginase expression and functionality significantly decreases post-differentiation, raising a concern if those levels could potentially drop even further after transplantation. This decrease could be a result of using the Ef1α promoter, which has been shown to drop in activity post-differentiation. Further studies are needed to investigate methods to enhance the arginase expression and functionality in both hiPSCs and their hepatocyte derivatives. Several strategies we have begun to focus on include targeting the endogenous hepato-specific Albumin gene for ArgO integration, investigating the use of other promoters, and modifying the ArgO cassette to include dual copies of arginase separated by a self-cleaving 2A peptide (p2A).

Additionally, we are investigating other hepatocyte differentiation protocols to enhance differentiation efficiency and generate a higher quantity and quality of pure hepatocyte-like cells. These additional steps are necessary as we look to

translate the results of this study to a mouse model of arginase deficiency. Successful demonstration of CRISPR/Cas9-mediated genetic modification of hiPSCs and restoration of ureagenesis in mouse models using corrected hiPSCs can provide a method that can be applied universally to correcting other forms of UCD and other single enzyme disorders.

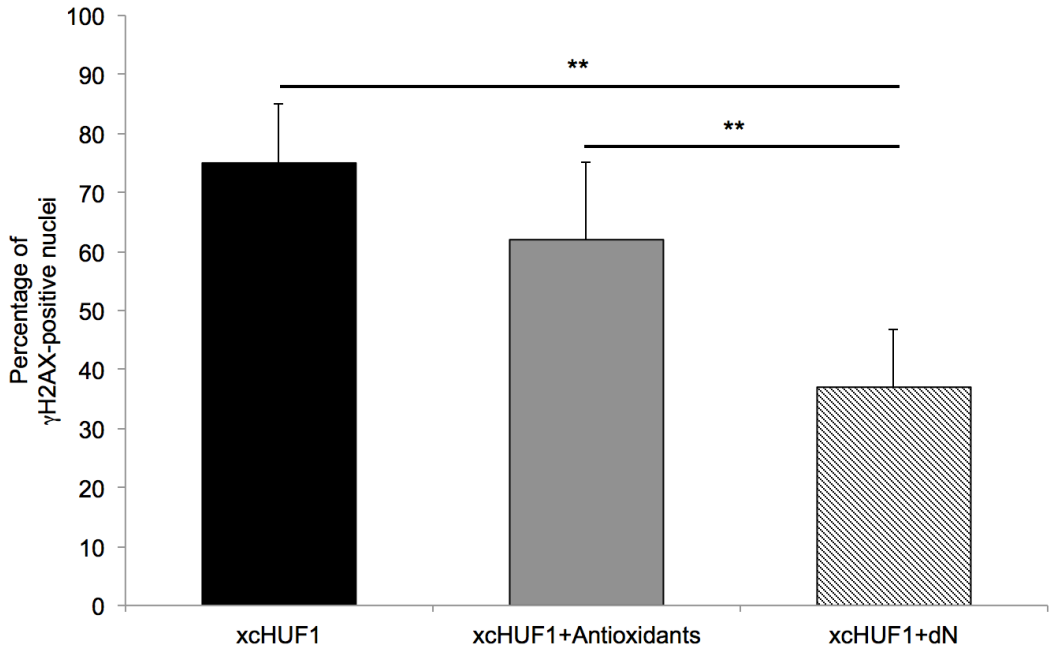

Supplementary Figure 1-1. Comparison of antioxidant and nucleoside supplementation

xcHUF1 hiPSCs were cultured for two weeks with either ascorbic acid or our nucleoside supplement for two weeks (n=50). hiPSCs that were cultured in dNs exhibited 40% less γH2AX-positive nuclei compared to those supplemented with antioxidants. Data are represented as means ± SD. **p<0.05 unpaired two-tailed t-test.

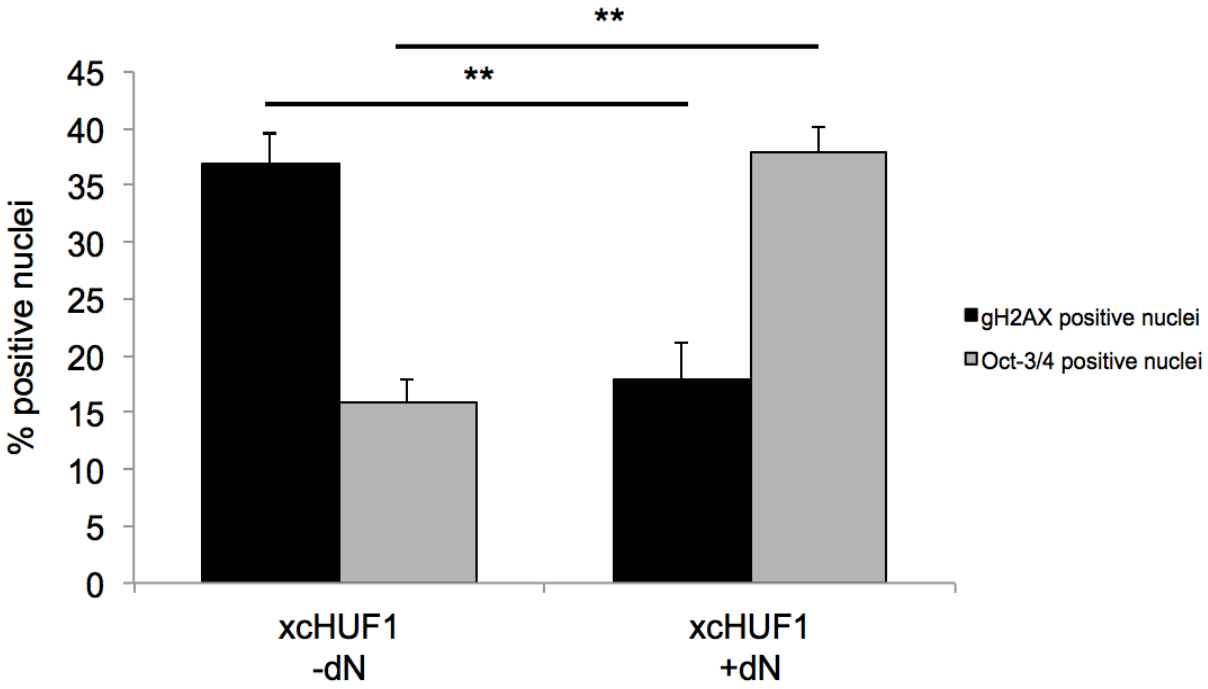

Supplementary Figure 1-2. dN supplementation increases Oct-3/4 expression during reprogramming

xcHUF1 fibroblasts were reprogrammed with or without dN supplementation. Three days after lentiviral transfection, fibroblasts supplemented with dNs exhibited higher levels of Oct-3/4 and lower levels of DSBs (n=50). Data are represented as means ± SD. **p<0.05 unpaired two-tailed t-test

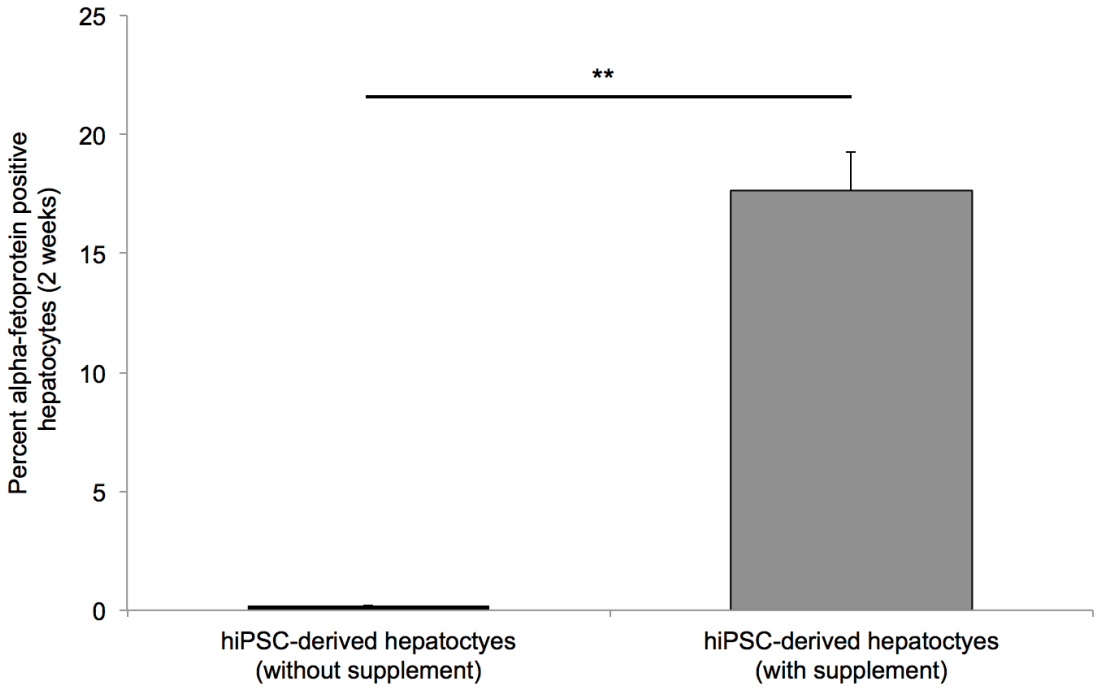

Supplementary Figure 1-3. AFP expression in hepatocyte-like cells with or without dN supplementation

Hepatocyte-like cells were maintained in culture two weeks post-differentiation with or without dN supplementation (n=50). Hepatocyte-like cells cultured with supplement maintained higher levels of AFP, with 17% of cells expressing AFP. AFP was detected via immunocytochemistry. Data are represented as means ± SD. **p<0.05 unpaired two-tailed t-test

References

1) Takahashi J., Tanabe K., Ohnuki M., Narita M, Ichisaka T., Tomoda K., Yamanaka S. Induction of pluripotent stem cells from adult human fibroblasts by defined factors. *Cell* 131:861-72 (2007).

2) Yu J., Vodyanik M.A., Smuga-Otto K., Antosiewicz-Bourget J., Frane J.L., Tian S., Nie J., Jonsdottir G.A., Ruotti V., Stewart R., Slukvin I.I., Thomson J.A. Induced pluripotent stem cells lines derived from human somatic cells. *Science* 318: 1917-1920 (2007).

3) Swistowski A., Peng J., Liu Q., Mali P., Rao M., Cheng L., Zheng X. Efficient generation of functional dopaminergic neurons from human induced pluripotent stem cells under defined conditions. *Stem Cells* 28: 1893-1904 (2010).

4) Song Z., Cai J., Liu Y., Zhao D., Yong J., Duo S., Song X., Guo Y., Zhao Y., Qin H., Yin X., Wu C., Chen J., Lu S., Ding M., Deng H. Efficient generation of hepatocyte-like cells from human induced pluripotent stem cells. *Cell Res* 19: 1233-1242 (2009).

5) Kanemura H., Go M., Shikamura M., Nishishita N., Sakai N., Kamao H., Mandai M., Morinaga C., Takahashi M., Kawamata S. Tumorigenicity studies of induced pluripotent stem cell (iPSC)-derived retinal pigment epithelium (RPE) for the treatment of age-related macular degeneration. *PLoS ONE* 9:e85336 (2014).

6) Jinek M., Chylinski K., Fonfara I., Hauer M., Doudna JA., Charpentier E. A programmable dual-RNA-guided DNA endonuclease in adapative bacterial immunity. *Science* 337(6096):816-21. (2012).

7) Flynn R., Grundmann A., Renz P., Hanseler W., James WS., Cowley SA., Moore MD. CRISP-mediated genotypic and phenotypic correction of a chronic granulomatous disease mutation in human iPS cells. *Exp Hematol* 43(10):838-48.e3 (2015).

8) Young CS., Hicks MR., Ermolova NV., Nakano H., Jan M., Younesi S., Karumbayaram S., Kuamagai-Cresse C., Wang D., Zack JA., Kohn DB., Nakano A., Nelson SF., Miceli MC., Spencer MF., Pyle AD. A single CRISPR-cas9 deletion strategy that targets the majority of DMD patients restores dystrophin function in hiPSC-derived muscle cells. *Cell Stem Cell* 18(4):533-40 (2016).

9) Hockemeyer D., Jaenisch R. Induced pluripotent stem cells meet genomic editing. *Cell Stem Cell* 18(5):573-86 (2016).

10) Marraffini LA., Sontheimer EJ. CRISPR interference: RNA-directed adaptive immunity in bacteria and archaea. *Nature Reviews* 11(3):181-90 (2010).

11) Mali P., Esvelt KM., Church GM. Cas9 as a versatile tool for engineering biology. *Nature Methods* 10(10):957-53 (2013).

12) Li S., Xue H., Long B., Sun L., Truong T., Liu Y. Efficient generation of hiPSC neural lineage specific knockin reporters using the CRISPR/Cas9 and Cas9 double nickase system. *J Vis Exp* 99:e52539 (2015).

13) Lee PC., Truong B., Vega-Crespo A., Hermann K., Kingman S., Tang JK, Chang KM., Wininger AE., Lam AK., Schoenberg BE., Cederbaum SD., Pyle AD., Byrne JA., Lipshutz GS. Restoring ureagenesis in hepatocytes by CRISPR/Cas9-mediated genomic addition to arginase-deficient induced pluripotent stem cells. *In Review* (2016).

14) Peterson SE., Loring JF. Genomic instability in pluripotent stem cells: implications for clinical applications. *JBC* 289:4578-84 (2013).

15) Martins-Taylor K., Xu R. Concise Review: genomic instability of human induced pluripotent stem cells. *Stem Cells* 30:22-27 (2012).

16) Weissbein U., Benvenisty N., Ben-David U. Genome maintenance in pluripotent stem cells. *JCB* 204:153-63 (2014).

17) Halazonetis TD., Gorgoulis VG., Bartek J. An oncogene-induced DNA damage model for cancer development. *Science* 319:1352-55 (2008).

18) Chung T., Thakar NY., Wolvetang EJ. Genetic and epigenetic instability of human pluripotent stem cells. *The Open Stem Cell Journal* 3:52-61 (2011).

19) Becker KA., Ghule PN., Therrien JA., Lian JB., Stein JL, van Wijnen AJ., Stein GS. Self-renewal of human embryonic stem cells is supported by a shortened G1 cell cycle phase. *J Cellular Physiol* 209:883-93 (2006).

20) Calder A., Roth-Albin I., Bhatia S., Pilquil C., Lee JH, Bhatia M., Levadoux-Martin M., McNicol J., Russell J., Collins T., Draper JS. Lengthened G2 phase indicates differentiation status in human embryonic stem cells. *Stem Cells and Development* 22:279-95 (2013).

21) Ghule PN., Medina R., Lengner CJ., Mandeville M., Qiao M., Dominski Z., Lian JB., Stein JL, van Wijnen AJ., Stein GS. Reprogramming the pluripotent cell cycle: restoration of an abbreviated G1 phase in human induced pluripotent (iPS) cells. *J Cell Physiol.* 226:1149-56 (2011).

22) Steinemann D., Gohring G., Schlegelberger B. Genetic instability of modified stem cells – a first step towards malignant transformation? *Am J Stem Cell* 2:39-51 (2013)

23) Mayshar Y., Ben-David U. Lavon N., Biancotti J., Yakir B., Clark AT., Plath K., Lowry WE., Benvenisty N. Identification and classification of chromosomal aberrations in human induced pluripotent stem cells. *Cell Stem Cell* 7(4)521-31 (2010).

24) Ji J., Sharma V., Qi S., Guarch ME., Zhao P., Luo Z, Fan W., Wang Y., Mbabaali F., Neculai D., Esteban MA., McPherson JD., Batada NN. Antioxidant supplementation reduces genomic aberrations in human induced pluripotent stem cells. *Stem Cell Reports* 2:44-51 (2014).

25) Luo L., Kawakatsu M., Guo C., Urata Y., Huang W., Ali H., Kitajima Y., Tanaka T., Goto S., Ono Y., Xin H., Hamano K., Li T. Effects of antioxidants on the quality and genomic stability of induced pluripotent stem cells. *Scientific Reports* 4:3779 (2014).

26) Noon AT., Goodarzi AA. 53BP1-mediated DNA double strand break repair: instert bad pun here. *DNA Repair (Amst)* 10:745-53 (2011).

27) Bester AC., Roniger M., Oren YS., Im MM., Sami D., Chaoat M., Bensimon A., Zamir G., Shewach DS., Kerem B. Nucleotide deficiency promotes genomic instability in early stages of cancer development. *Cell* 145:435-46 (2011).

28) Lecona E., Fernandez-Capetillo O. Replication stress and cancer: it takes two to tango. *Exp Cell Res* 329(1):26-34 (2014).

29) Jones RM., Mortusewics O., Afzal I., Lorvellec M., Garcia P., Helleday T., Peterman E. Increased replication initiation and conflicts with transcription underlie Cyclin E-induced replication stress. *Oncogene* 32(32):3744-53 (2013).

30) Bartek J., Lukas J. Chk1 and Chk2 kinases in checkpoint control and cancer. *Cancer Cell* 3(5):421-29 (2003).

31) Ruiz S., Lopez-Contreras AJ., Gabut M., Marion RM., Gutierrez-Martinez P., Bua S., Ramirez O., Olalde I., Rodrigo-Perez S., Li H., Marques-Bonet T., Serrano M., Blasco MA., Batada NN., Fernandez-Capetillo O. Limiting replication stress during somatic cell reprogramming reduces genomic instability in induced pluripotent stem cells. *Nat Commun* 6:8036 (2015).

32) Mathews CK. Deoxyribonucleotide metabolism, mutagenesis, and cancer. *Nat Rev Cancer* 15(9): 528-39 (2015).

33) Aird KM., Zhang G., Tu Z., Bitler BG., Garipov A., Wu H., Wei Z., Wagner SN., Herlyn M., Zhang R. Suppression of nucleotide metabolism underlies the establishment and maintenance of oncogene-induced senescence. *Cell Rep* 3(4):1252-65 (2013).

34) Nathanson DA., Armijo AL., Tom M., Li Z., Dimitrova E., Austin WR., Nomme J., Campbell DO., Ta L., Le TM., Lee JT., Darvish R., Gordin A., Wei L., Liao HI., Wilks M., Martin C., Sadeghi S., Murphy JM., Boulos N., Phelps ME., Faull KF., Herschman HR., Jung ME., Czernin J., Lavie A., Radu CG. Co-targeting of convergent nucleotide biosynthetic pathways for leukemia eradication. *J Exp Med* 211(3):473-86 (2014).

35) Rodriguez-Serrano F., Alvarez P., Caba O., Picon M., Marchal JA., Peran M., Prados J., Melguizo C., Rama AR., Boulaiz H., Aranega A. Promotion of human adipose-derived stem cell proliferation mediated by exogenous nucleosides. *Cell Bio Int* 34(9):917-24 (2010).

36) Wang J, Hao J, Bai D, Gu Q, Han W, Wang L, Tan, Y, Xia L, Xue K, Han P, Liu Z, Jia Y, Wu J, Liu L, Wang L, Li W, Liu Z, Zhou Q. Generation of clinical-grade human induced pluripotent stem cells in xeno-free conditions. *Stem Cell Res Ther* 6:233 (2015).

37) Burrell RA, McClelland SE, Endesfelder D, Groth P, Weller MC, Shaikh N, Domingo E, Kanu N, Dewhurst SM, Gronroos E, Chew SK, Rowan AJ, Schenk A, Sheffer M, Howell M, Kschischo M, Behrens A, Helleday T, Bartek J, Tomlinson IP, Swanton C. Replication stress links structural and numerical cancer chromosomal instability. *Nature* 494:492-96 (2013).

38) Heng HQ, Regan SM, Guo L, Ye C. Why is it crucial to analyze non clonal chromosome aberrations or NCCAs? *Mol Cytogenet* 9:15 (2016).

39) Summar ML., Koelker S., Freedenberg D., Le Mons C., Haberle J., Lee HS., Kirmse B. The incidence of urea cycle disorders. *Mol Genet Metab* 110:179-80 (2013).

40) Ah Mew N., Lanpher BC., Gropman A., Chapman KA., Simpson KL. Urea Cycle Disorders, C., Summar ML. Urea Cycle Disorders Overview. *GeneReviews(R)* (1993).

41) Deignan JL, Cederbaum SD., Grody WW. Contrasting features of urea cycle disorders in human patients and knockout mouse models. *Mol Genat Metab* 93:7-14 (2008).

42) Foschi FG., Morelli MC., Savini S., Dall'Aglio AC., Lanzi A., Cescon M., Ercolani G., Cucchetti A., Pinna AD., Stefanini GF. Urea cycle disorders: a case report of a successful treatment with liver transplant and a literature review. *World J Gastroenterol* 21:4063-63 (2015).

43) Uchino T., Snyderman SE., Lambert M., Qureshi IA., Shapira SK., Sansaricq C., Smit LM., Jakobs C., and Matsuda I. Molecular basis of phenotypic variation in patients with argininemia. *Hum Genet 96*, 255-260 (1995).

44) Cederbaum SD., Yu H., Grody WW., Kern RM., Yoo P., Iyer RK. Arginases I and II: do their functions overlap? *Mol Genet Metab* 81 Suppl1:S38-44 (2004).

45) Hu C., Kasten J., Park H., Bhargava R., Tai DS., Grody WW., Nguyen QG., Hauschka SD., Cederbaum SD., Lipshutz GS. Myocyte-mediated arginase expression controls hyperargininemia but not hyperammonemia in arginase-deficient mice. *Mol Ther* 22:1792-1802 (2014).

46) Jain-Ghai S., Nagamani SC., Blaser S., Siriwardena K., and Feigenbaum A., (2011). Arginase I deficiency: severe infantile presentation with hyperammonemia: more common than reported? *Mol Genet Metab* 104:107-111 (2011).

47) Kasten J., Hu C., Bhargava R., Park H., Tai D., Byrne JA., Marescau B., De Deyn PP., Schlichting L., Grody WW. Lethal phenotype in conditional late-onset arginase 1 deficiency in the mouse. *Mol Genet Metab* 110:222-230 (2013)

48) Luiking YC., Engelen MP, Deutz NE. Regulation of nitric oxide production in health and disease. *Curr Opin Clin Nutr Metab Care* 13:97-104 (2010).

49) Byrne JA., Nguyen HN, Reijo Pera RA. Enhanced generation of induced pluripotent stem cells from a subpopulation of human fibroblasts. *PLoS One* 4:e7118 (2009).

50) Lowry WE., Richter L., Yachechko R., Pyle AD., Tchieu J., Sridharan R., Clark AT., Plath K. Generation of human induced pluripotent stem cells from dermal fibroblasts. *Proc Natl Acad Sci* 105:2883-888 (2008).

51) Takahashi K., Tanabe K., Ohnuki M., Narita M., Ichisaka T., Tomoda K., Yamanaka S. Induction of pluripotent stem cells from adult human fibroblasts by defined factors. *Cell* 131:861-72 (2007).

52) Takahashi K., Yamanaka S. Induction of pluripotent stem cells from mouse embryonic and adult fibroblast cultures by defined factors. *Cell* 126:663-76 (2006).

53) Yu J. Vodyanik MA. Smuga-Otto K., Antosiewicz-Bourget J., Frane JL., Tian S., Nie J., Jonsdottir GA., Ruotti V., Stewart R. Induced pluripotent stem cell lines derived from human somatic cells. *Science* 318:1917-20 (2007).

54) Chen YF., Tseng CY., Wang HW., Kuo HC., Yang VW., Lee, OK. Rapid generation of mature hepatocyte-like cells from human induced pluripotent stem cells by an efficient three-step protocol. *Hepatology* 55:1192-203 (2012).

55) Song Z., Cai J., Liu Y., Zhao D., Yong J., Duo S., Song X., Guo Y., Zhao Y., Qin H. Efficient generation of hepatocyte-like cells from human induced pluripotent stem cells. *Cell Res* 19: 1233-42 (2009).

56) Zhang Z., Huang B., Gao F., Zhang R. Impact of immune response on the use of iPSCs in disease modeling. *Curr Stem Cell Res Ther* 10:236-44 (2015).

57) Karumbayaram S., Lee P., Azghadi SF., Cooper AR., Patterson M., Kohn DB., Pyle A., Clark A., Byrne JA., Zack JA. From skin biopsy to neurons through a pluripotent intermediate under good manufacturing practice protocols. *Stem Cells Transl Med* 1:36-43 (2012).

58) Durruthy-Durruthy J., Briggs SF., Awe J., Ramathal CY., Karumbayaram S., Lee PC., Heidmann JD., Clark A., Karakikes I., Loh KM. Rapid and efficient conversion of integration-free human induced pluripotent stem cells to GMP-grade culture conditions. *PLoS One* 9:e94231 (2014).

59) Sommer CA., Stadtfeld M., Murphy GJ., Hochedlinger K., Kotton DN., Mostoslavsky G. Induced pluripotent stem cell generation using a single lentiviral stem cell cassette. *Stem Cells* 27:543-49 (2009).

60) Somers A., Jean JC., Sommer CA., Omari A., Ford CC., Mills JA., Ying L., Sommer AG., Jean JM., Smith BW. Generation of transgene-free lung disease-specific human induced pluripotent stem cells using a single excisable lentiviral stem cell cassette. *Stem Cells* 28:1728-40 (2010).

61) Bachmann C. Outcome and survival of 88 patients with urea cycle disorders: a retrospective evaluation. *Eur J Pediatr* 162:410-16.

62) Enns GM., Berry SA., Berry GT., Rhead WJ., Brusilow SW., and Hamosh A. Survival after treatment with phenylacetate and benzoate for urea-cycle disorders. *N Engl J Med* 356:2282-92 (2007).

63) Gau CL., Rosenblatt RA., Cerullo V., Lay FD., Dow AC., Livesay J., Brunetti-Pierri N., Lee B., Cederbaum SD., Grody WW. Short-term correction of arginase deficiency in a neonatal murine model with a helper-dependent adenoviral vector. *Mol Ther* 17:1155-1163 (2009).

64) Meyberg J., Hoffmann GF. Liver, liver cell and stem cell transplantation for the treatment of urea cycle defects. *Mol Genet Metab* 100 Suppl 1:S77-83 (2010).

65) Strulovici Y. Leopold PL., O'Connor TP. Pergolizzi RG., Crystal RG. Human embryonic stem cells and gene therapy. *Mol Ther* 15:850-66 (2007).

66) Gerecht-Nir S., Itskovitz-Eldor J. Human embryonic stem cells: a potential source for cellular therapy. *Am J Transplant* 4 Suppl 6:51-57 (2004).

67) Liu H., Kim Y., Sharkis S., Marchionni L., Jang YY. In vivo liver regeneration potential of human induced pluripotent stem cells from diverse origins. *Sci Transl Med* 3:82ra39 (2011).

68) Schambach A., Cantz T., Baum C., Cathomen T. Generation and genetic modification of induced pluripotent stem cells. *Expert Opin Biol Ther*. 10:1089-1103 (2010).

69) Giudice A., Trounson A. Genetic modification of human embryonic stem cells for the derivation of target cells. *Cell Stem Cell* 2:422-33 (2008).

70) Musunuru K., Genome editing of human induced pluripotent stem cells to generate human cellular disease models. *Dis Model Mech* 6:896-904 (2013).

71) Yusa K., Rashid ST., Strick-Marchand H., Varela I., Liu PQ., Paschon DE., Miranda E., Ordonez A., Hannan NR., Rouhani FJ. Targeted gene correction of alpha1-antitrypsin deficiency in induced pluripotent stem cells. *Nature* 478:391-94 (2011).

72) Lee EK., Hu C., Bhargava R., Ponnusamy R., Park H., Novicoff S., Rozengurt N., Marescau B., De Deyn P. Stoute D., Schlichting L., Grody WW., Cederbaum SD., Lipshutz GS. AAV-based gene therapy prevents neuropathy and results in normal cognitive development in the hyperargininemic mouse. *Gene Ther.* 20(8):785-96 (2013).

73) Hu C., Tai DS., Park H., Cantero G., Chan E., Yudkoff M., Cederbaum SD., Lipshutz GS. Minimal ureagenesis is necessary for survival in the murine model of hyperargininemia treated by AAV-based gene therapy. *Gene Ther* 22:111-115 (2015).

74) Lee EK., Hu C., Bhargava R., Rozengurt N., Stout D., Grody WW., Cederbaum SD., Lipshutz GS. Long-term survival of the juvenile lethal arginase-deficient mouse with AAV gene therapy. *Mol Ther* 20:1844-1851 (2012).

75) Silverman LJ., Kelly WN., Palella TD. Genetic analysis of human hypoxanthine-guanine phosphoribosyltransferase deficiency. *Enzyme* 38:36-44 (1987).

76) Liao S., Tammaro M., Yan H. Enriching CRISPR-Cas9 targeted cells by co-targeting the HPRT gene. *Nucleic Acids Res* 43:e134 (2015).

77) Swann PF., Waters TR., Moulton DC., Xu YZ., Zheng Q., Edwards M., Mace R. Role of postreplicative DNA mismatch repair in the cytotoxic action of thioguanine. *Science* 273:1109-11 (1996).

78) Narsinh KH., Wu JC. Gene correction in human embryonic and induced pluripotent stem cells: promises and challenges ahead. *Mol Ther* 18:1061-63 (2010).

79) Shaw-White JF., Denko N., Albers L., Doetschman TC., Stringer JR. Expresion of the lacZ gene targeted to the HPRT locus in embryonic stem cells and their derivatives. *Transgenic Res* 2:1-13 (1993).

80) Hong S., Hwang DY., Yoon S., Isacson O., Ramezani A., Hawley RG., Kim KS. Functional Analysis of various promoters in lentiviral vectors at different stages of in vitro differentiation of mouse embryonic stem cells. *Mol Ther* 15:1630-39 (2007).

81) Bhatia SN., Underhill GH., Zaret KS., Fox IJ. Cell and tissue engineering for liver disease. *Sci Transl Med* 6:245sr242 (2014).

82) Soltys KA., Soto-Gutierrez A., Nagaya M., Baskin KM., Deutsch M., Ito R., Shneider BL., Squires R., Vockley J., Guha C., Roy-Chowdhury J., Strom SC., Platt JL, Fox IJ. Barriers to the successful treatment of liver disease by hepatocyte transplantation. *J Hepatol* 53:769-74 (2010).

83) Fox IJ., Chowdhury JR., Kaufman SS., Goertzen TC., Chowdhury NR., Warkentin PI., Dorko K., Sauter BV., Strom SC. Treatment of the Criger-Najjar syndrome type I with hepatocyte transplantation. *N Engl J Med* 338:1422-1426.

84) Puppi J., Tan N., Mitry RR., Hughes RD., Lehec S., Mieli-Vergani G., Karani J., Champion MP., Heaton N., Mohamed R., Dhawan A. Hepatocyte transplantation followed by auxiliary liver transplantation-a novel treatment for ornithine transcarbamylase deficiency. *Am J Transplant* 8:452-457 (2008).

85) Dhawan A., Mitry RR., Hughes RD., Lehec S., Terry C., Bansal S., Arya R., Wade JJ., Verma A., Heaton ND., Rela M., Mieli-Vergani G. Hepatocyte transplantation for inherited factor VII deficiency. *Transplantation* 78:1812-14 (2004).

86) Horslen SP., McCowan TC., Goertzen TC., Warkentin PI., Cai HB., Strom SC., Fox IJ. Isolated hepatocyte transplantation in an infant with a severe urea cycle disorder. *Pediatrics* 111:1262-67 (2003).

87) Muraca M., Gerunda G., Neri D., Vilei MT., Granato A., Feltracco P., Meroni M., Giron G., Burlina AB. Hepatocyte transplantation as a treatment for glycogen storage disease type 1a. *Lancet* 359:317-18 (2002).

88) Sokal EM., Smets F., Bourgois A., Van Maldergem L., Buts JP., Reding R., Bernard Otte J., Evrard V., Latinne D., Vincent MF., Moser A., Soriano HE. Hepatocyte transplantation in a 4-year old girl with peroxisomal biogenesis disease: technique, safety, and metabolic follow-up. *Transplantation* 76(4):735-8 (2003).